Medicinal Chemistry Research (2019) 28:1010–1026
https://doi.org/10.1007/s00044-019-02355-z

MEDICINAL CHEMISTRY RESEARCH

ORIGINAL RESEARCH

Design, synthesis and biological evaluation of novel indone derivatives as selective ERβ modulators

Xi-Xi Liu[1] · Mei-Lin Tang[1,4] · Chen Zhong[1] · Yun Tang[3] · Jian-Ming Yu[1] · Xun Sun[1,2]

Received: 26 November 2018 / Accepted: 30 April 2019 / Published online: 17 May 2019

Abstract

To reduce the endometrial toxicity and improve the efficacy of current selective estrogen receptor modulators used in breast cancer treatment by enhancing ERβ selectivity, inspired by active resveratrol oligomer, a series of analogs (**5a–f**, **6a–b**, **7a–d**, **8a–d**) were designed, synthesized and biologically evaluated. Among them, the chiral indone analog (2*R*,3*R*)**-8a** exhibited best antiproliferative activity against both breast cancer cell lines (MDA-MB-231 and MCF-7) and better safety profile on uterus than tamoxifen. Analog (2*R*,3*R*)**-8a** demonstrated good binding affinity and selectivity toward ERβ, which was further proved by both molecular docking and radiometric competitive binding assay. Other studies for (2*R*,3*R*)**-8a** also have been explored including cell cycle and apoptosis evaluation and in vitro metabolic stability studies. These results demonstrated that (2*R*,3*R*)**-8a** could be a promising lead compound for future exploration of selective ERβ anti-breast cancer agents.

Keywords Resveratrol oligomer · ERβ · Breast cancer · SERM

Introduction

Breast cancer has become a great threat to females, accounting for 24.2% of all cancer cases in women and causing 626,679 deaths worldwide in 2018, according to the global cancer statistics 2018 (Bray et al. 2018). Surgery, chemotherapy, and newly antibody therapies like HER2-targeted therapy have been used to cure different types of breast cancer (Figueroa-Magalhães et al. 2014), but still along with various drawbacks, such as high rates of recurrence, metastasis, severe toxicity, and drug resistance. Selective estrogen receptor modulators (SERMs) (Fig. 1) are widely used in preventing or treating estrogen-related diseases including breast cancer and osteoporosis (Howell and Evans 2013). However, despite their promising effectiveness and widely usage, SERMs still suffer from unsolved safety issues. For example, tamoxifen enhances the risk of endometrial cancer and liver damage, whereas raloxifene may increase the chance of stroke (Jordan 2004; Ellis et al. 2015). Since the discovery of the two subtypes, ERα and ERβ (Mosselman et al. 1996; Paterni et al. 2014), the lack of ER subtype and tissue selectivity of these SERMs has been considered to be responsible for most of the side effects. So far, most preliminary SERM studies were focused on the investigation of ERα-selective agents. However, disadvantages have been observed for ERα-selective SERMs such as causing severe side effects in ERα highly expressed tissues including liver, uterus, and cardiovascular system (Skliris et al. 2008). Meanwhile, the tissue distribution of ERβ is quite different from ERα. ERβ expresses very few in liver and uterus, which may reduce the influence on these tissues by selective ERβ modulators (Skliris et al. 2008; Dotzlaq 1997). Thus, ERβ-selective ligands could be utilized as novel anti-breast cancer agents

Supplementary Information The online version of this article (https://doi.org/10.1007/s00044-019-02355-z) contains supplementary material, which is available to authorized users.

✉ Xun Sun
sunxunf@shmu.edu.cn

1 Department of Natural Products Chemistry, School of Pharmacy, Fudan University, Shanghai, China

2 The Institutes of Integrative Medicine of Fudan University, Shanghai, China

3 Shanghai Key Laboratory of New Drug Design, School of Pharmacy, East China University of Science and Technology, Shanghai, China

4 State Key Laboratory of Molecular Engineering and Institutes of Biomedical Sciences, Fudan University, 220 Handan Road, Shanghai 200433, China

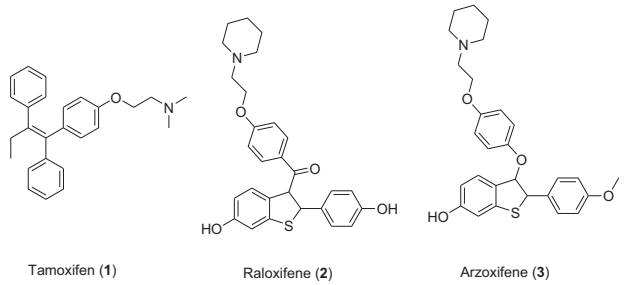

Fig. 1 Selective estrogen receptor modulators (SERMs)

with potentially less side effects (Fox et al. 2008; Hartman et al. 2009; Ström et al. 2004).

Previously, Paul Mak et al. (2006) reported that the natural compound Apigenin can suppress breast cancer cell growth and induce apoptosis through ERβ. Interestingly, natural compound resveratrol is a polyphenol, which widely exists in several kinds of plants, and its anticancer activity has been confirmed by many studies (Bishayee 2009). Many efforts have been done in our group in the past years and lots of oligomers have been synthesized including oligomer derivatives from *Caragana sinica* acting as phytoestrogens (Luo et al. 2001; Ma et al. 2010; Sun et al. 2006, 2007; Zhu et al. 2008; Zhong et al. 2011, 2013; Wang et al. 2015; Tang et al. 2016). After biological evaluation of these derivatives, it was found that isopaucifloral F (Jordan 2004) (Fig. 2) showed good in vivo anti-osteoporosis activity in rat, preferring ERβ activity in yeast two-hybrid assay and low toxicity (Hao et al. 2015). However, isopaucifloral F (Jordan 2004) did not show anticancer activity in MTT assay on human breast cancer cell lines MCF-7 and MDA-MB-231. Based on the general structural formula brought up by Grese et al. (1997), it was speculated that both *trans* 1,2-stilbene-like core structure and a dialkylamine side chain could be pivotal in SERMs for their anticancer activity. Isopaucifloral F (Jordan 2004) possesses a *trans* 1,2-stilbene-like core structure but lacks the key dialkylamine side chain. Thus, incorporated a dialkylaminoethoxyphenyl substituent into isopaucifloral F (Jordan 2004) may enhance its anticancer activity. According to previous studies, it was found that piperidine or pyrrolidine may contribute to achieve better antagonist activity (Grese et al. 1997). Therefore, when designing the different dialky-substituents on the basic amine of the side chain, we chose piperidine and its derivatives as the source for basic amine.

To further enhance ERβ selectivity, we compared isopaucifloral F (Jordan 2004) structure with ERα and ERβ ligand model developed by Katzenellenboen's group (Meri De Angelis et al. 2005). Isopaucifloral F (Jordan 2004) has compact core structure and less substituents, which is more consistent with ERβ ligands model. Herein, two strategies were applied to design novel analogs by maintaining or reducing hydroxyl group(s) on phenyl rings (analogs **5** and **7**), which may strengthen its good binding affinity to ERβ or methylating hydroxyl group(s) on phenyl rings (analogs **6** and **8**), which may increase the metabolic stability. Thus, total 16 novel analogs (**5a–f**, **6a–b**, **7a–d**, and **8a–d**) were designed and synthesized and their biological activities were evaluated.

Chemistry

The target compounds **5**–**8** were synthesized by following the procedure described in Scheme 1. Commercially available 1-chloromethyl-4-methoxybenzene and magnesium were used to produce a Grignard reagent that reacted with chlorodiphenyl phosphine and then was oxidized to give (4-methoxybenzyl) diphenylphosphine oxide (Dotzlaq 1997). After de-methylation, the obtained intermediate **10** reacted with 2-(benzyloxy)ethyl-4-methylbenzenesulfonate to give **11** in 78% yield. Compound **12** was achieved by debenzylation with $AlCl_3$ condition in almost quantative yield. Direct replacement of tosyl group with various amines provided **14a–f** in 52–81% yields. Subjected **14a–f** to substituted benzils **15** or **16** gave corresponding α, β-unsaturated ketone intermediates **17a–f** or **18a–f** as a mixture of *E*- and *Z*-isomer via Wittig–Horner reaction. Compounds (**5a–f**, **6a–b**, **7a–d**, and **8a–d**) were synthesized via Nazarov cyclization using conditions either $BF_3{\cdot}Et_2O$ or BBr_3. In order to study the effect of stereochemistry, enantiomerically enriched compounds (2*R*,3*R*)-**8a** and (2*S*,3*S*)-**8a** were also separated from its racemic form by Daicel Chiral Technologies (China) Co., Ltd. using high-performance liquid chromatography (HPLC) and chiral column. The absolute configurations were determined by the circular dichroism (CD) spectra method. The same CD spectral patterns were observed among previous chiral synthesized compounds and (2*R*,3*R*)-**8a**, indicating that they have identical stereochemistry that confirmed the absolute configurations of two enantiomerically enriched compounds (Tang et al. 2016).

Results and discussion

Cytotoxicity against human breast cancer cells

To evaluate the anticancer activity of designed compounds, two cancer cell lines MCF-7 (expressing both in ERα and ERβ) and MDA-MB-231 (expressing only in ERβ) were chosen to study their in vitro cytotoxicity using standard MTT assay (Dotzlaq 1997; Mak et al. 2006). The ER expression

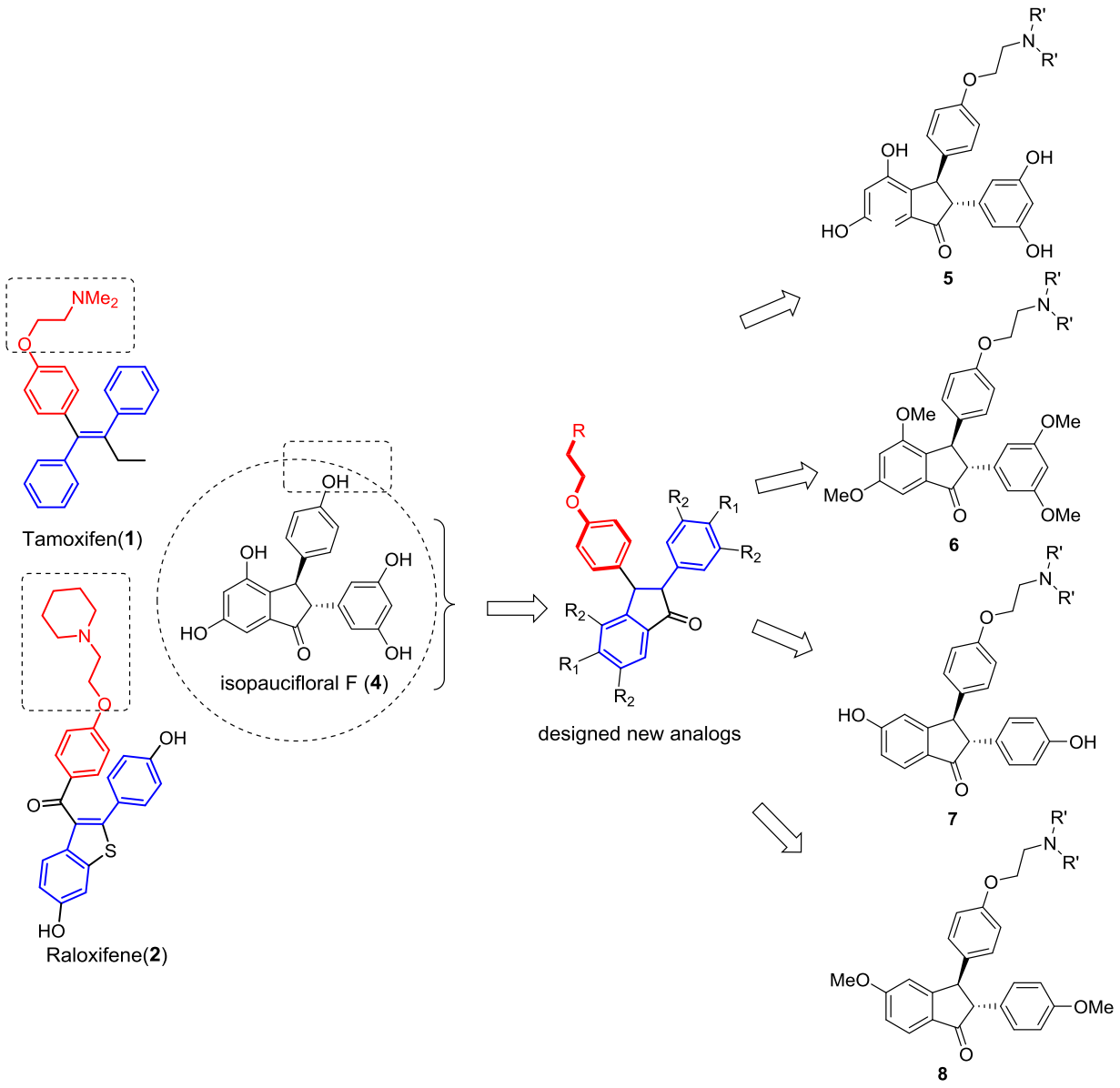

Fig. 2 Strategy for designing new analogs **5**–**8**

model of the two cell lines was confirmed by western blot analysis (Fig. 3). The activity is expressed as the concentration of drug inhibition at 50% cell growth (IC_{50}) and the data are presented in Table 1. Tamoxifen, raloxifene and isopaucifloral F were used as controls. Initially, analogs **5**, **6**, and **7** were taken into examination. The results showed similar trends in all two cell lines. Isopaucifloral F (Jordan 2004) and analogs **5**, which have four hydroxyls did not show any anticancer activity for both MDA-MB-231 and MCF-7 cell lines. However, **7a–b** (with two hydroxyls) and **6a–b** (with four methoxys) showed slightly improved activity, whereas **7c–d** were inactive for both cell lines even after 72 h treatment. The results indicated that either methylation of hydroxyl groups or reduction of hydroxyl groups on the A and C rings may have positive influence on the anticancer activity. Based on these results, further structure–activity relationship study was carried out to design new analogs **8** with methoxyl substituted on R_2. As speculated, analogs **8** did show the best inhibitory activity in four series.

As rationalized, the side chains of alkylamino groups do affect the biological activities. Overall, compounds with piperidine ring (**6a** and **8a**) displayed better activities against two cell lines, whereas compounds with morpholine ring (**7c** and **8d**) did not show any or weaker activity. Compared with control drugs, tamoxifen and raloxifene, compounds **8a**, **8b**, and **8c** showed similar or improved activity. Especially, analog **8a** exhibited 2.2- and 1.4-fold more potent than tamoxifen and 2.8- and 1.8-fold more

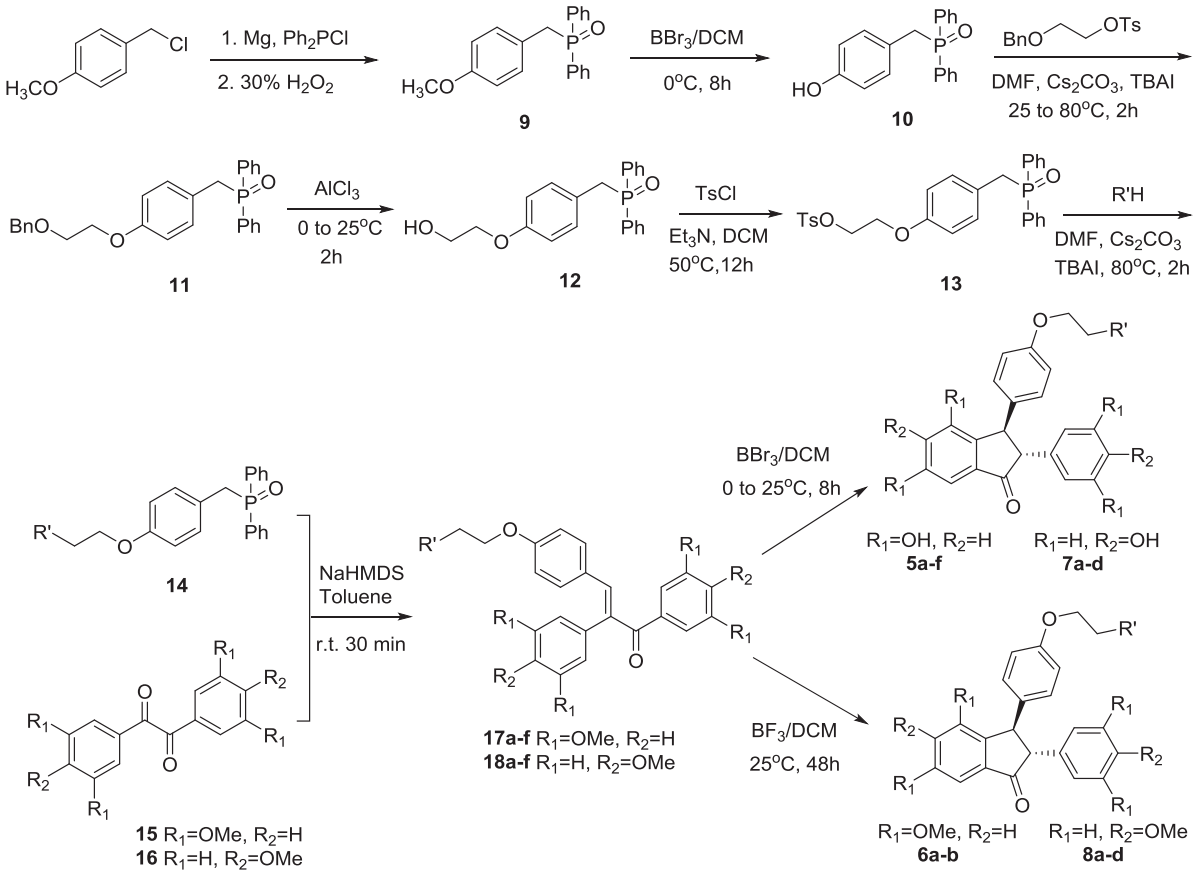

Scheme 1 The syntheses of new analogs of **5a–f**, **6a–b**, **7a–d**, and **8a–d**

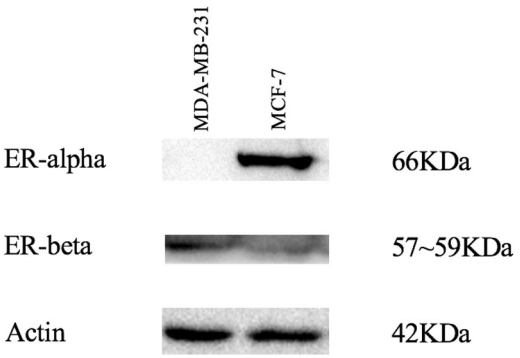

Fig. 3 The expression of ERα and ERβ in MCF-7 and MDA-MB-231 was shown by western blot analysis. No ERα was detected in MDA-MB-231, whereas both ERα and ERβ were detected in MCF-7

potent than raloxifene against MDA-MB-231 and MCF-7 cell line, respectively, after 72 h treatment.

As **8a** had optical enantiomers, to further study whether the chiral structure affected the anticancer activity of the compounds, we separated **8a** with HPLC and chiral column to give (2*S*,3*S*)-**8a** ($[\alpha]_D^{20} = +151.5$ ($c = 0.4$ in MeOH)) and (2*R*,3*R*)-**8a** ($[\alpha]_D^{20} = -151.5$ ($c = 0.4$ in MeOH). Interestingly, the separated chiral compounds showed the difference on activities. Analog (2*R*,3*R*)-**8a** was more potent than (2*S*,3*S*)-**8a** against both MDA-MB-231 (3.94 vs. 7.45 μM) and MCF-7 (7.16 vs. 11.64 μM) cell line after 72 h treatment. This indicated that stereochemistry of compounds does influence the antiproliferative effect on ERβ expressed cell lines.

Docking analysis

To explore the ER subtype selectivity of active compounds and elucidate the binding model of active compounds with ERβ receptor, molecule docking analysis was undertaken using Schrodinger software (Schrödinger version 9.3, Schrödinger, LLC, New York, NY). The crystal structure of human ER5β ligand-binding domain (LBD) in complex with 4-hydroxytamoxifen (PDB ID: 2FSZ) and estrogen receptor α LBD in complex with raloxifene (PDB ID: 2JFA) were used for the docking. The protein was prepared using Maestro module of Schrodinger software. During protein preparation, correct bond orders were assigned and hydrogen along with other missing atoms were added. Residues and charges were assigned to atoms using OPLS-AA force field and the co-crystallized waters were retained for docking. The

Table 1 New compound in vitro cytotoxicity on human breast cancer cell lines MDA-MB-231 and MCF-7

Compound NO.	R_1	R_2	R′	IC_{50} (μM) [a]			
				MDA-MB-231		MCF-7	
				48 h	72 h	48 h	72 h
5a	OH	H	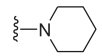	NA	NA	NA	NA
5b	OH	H		NA	NA	NA	NA
5c	OH	H		NA	NA	NA	NA
5d	OH	H		NA	NA	NA	NA
5e	OH	H		NA	NA	NA	NA
5f	OH	H	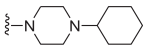	NA	NA	NA	NA
6a	OMe	H	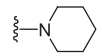	40.78 ± 2.51	11.82 ± 1.18	76.89 ± 7.59	61.49 ± 8.99
6b	OMe	H	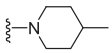	NA	19.19 ± 2.31	NA	259.47 ± 15.25
7a	H	OH	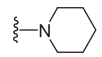	NA	41.91 ± 5.06	NA	NA
7b	H	OH	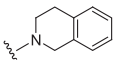	NA	43.86 ± 3.84	NA	30.75 ± 2.60
7c	H	OH	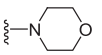	ND	ND	NA	NA
7d	H	OH		ND	ND	NA	NA
8a	H	OMe	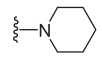	18.50 ± 1.95	6.00 ± 0.11	11.72 ± 1.99	7.68 ± 0.67
8b	H	OMe	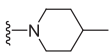	96.84 ± 5.42	25.78 ± 2.51	14.61 ± 3.91	8.40 ± 1.34
8c	H	OMe	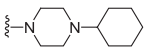	24.91 ± 1.43	16.48 ± 1.34	24.43 ± 1.10	9.80 ± 0.02
8d	H	OMe		NA	NA	139.94 ± 7.51	77.80 ± 5.47
raloxifene				53.25 ± 7.05	16.76 ± 1.15	21.24 ± 3.32	13.69 ± 2.60
tamoxifen				25.56 ± 1.25	13.06 ± 0.60	16.94 ± 0.66	9.51 ± 0.41
isopaucifloral F				NA	NA	NA	NA
(2*R*, 3*R*)-**8a**				12.32 ± 0.88	3.94 ± 0.29	9.09 ± 0.90	7.16 ± 0.54
(2*S*, 3*S*)-**8a**				19.66 ± 1.20	7.45 ± 0.33	19.05 ± 2.00	11.64 ± 1.09

NA not active, means IC50 cannot be calculated from MTT assay data; *ND* not determined

[a]Results were showed as means ± SD ($n = 3$) of at least three independent experiments

docking was done using Glide module of the Schrodinger software. The docking grid was generated using co-crystallized ligand (4-hydroxytamoxifen) as grid center with default settings. The ligands were sketched in Maestro module of Schrodinger software and were prepared using Ligprep module of Schrodinger software. The docking was performed with standard precision mode of Glide.

Compounds with strong activity against breast cancer cell lines were examined. Compound (2*R*,3*R*)-**8a** had better selectivity (ERβ/α = 1.93) than tamoxifen (ERβ/α = 0.89) (Table 2). Also, (2*R*,3*R*)-**8a** achieved good glide score with ERβ (glide score = −9.203) (Table 2). The docking results for (2*R*,3*R*)-**8a** showed a similar binding mode as 4-hydroxytamoxifen in ERβ-binding site, and the best pose was selected on the basis of the best docking score. The indone scaffold fitted into the hydrophobic pocket consists of Ile373 and Met336 residues, which distinguish ERβ from ERα (Gim et al. 2014). The methoxyl groups of the molecule formed hydrogen-bonding interactions with His475 and Arg346 and the ππ stacking interaction was also observed between 4-methoxylphenyl and Phe356. Further, the nitrogen atom of the piperidine group on (2*R*,3*R*)-**8a** had an electrostatic interaction with Asp303 (Fig. 4).

ER-binding affinity

Based on the result of the MTT assay and molecule docking, the most-effective compounds were chosen to investigate their binding affinity and selectivity to ERα and ERβ by a radiometric competitive binding assay (Table 3). All compounds showed better selectivity for ERβ than ERα. In particular, (2*R*,3*R*)-**8a** exhibited 6.98 times higher ERβ-binding affinity than ERα. The ERβ-binding results exhibited good consistency with the cytotoxicity results. Compound (2*R*,3*R*)-**8a** displayed better binding affinity than its counterpart enantiomer, which indicates that stereochemistry configurations have significant effects on receptor–ligand interactions. Compound (2*R*,3*R*)-**8a**, with the highest binding affinity among tested compounds, the IC_{50} value for ERβ was determined to be 0.513 μM.

Table 2 Docking results of active compounds (**8a** and **8c**) and ERs

Compound	Glide score		*β/α*
	ERα	ERβ	
(2*R*, 3*R*)-**8a**	−4.76	−9.20	1.93
(2*S*, 3*S*)-**8a**	−3.87	−5.98	1.54
(2*R*, 3*R*)-**8c**	–	−3.610	–
(2*S*, 3*S*)-**8c**	−3.44	−3.49	1.01
Tamoxifen	−12.96	−11.54	0.89

Oil/water partition coefficient assessment

The ability of organic chemicals to elicit certain therapeutic effect is strongly influenced by the partitioning tendency of these chemicals between the organism and water. The oil/water partition coefficient (log P) could be expressed as a ratio of n-octanol solubility to aqueous solubility. We determined the log *P* value of 2 in n-octanol/water at 37 °C. The result showed that (2*R*,3*R*)-**8a** has an appropriate oil/water partition coefficient (log $P = 2.3365$, $R^2 = 0.9999$), According to the Lipinski's rule of five (Lipinski et al. 2001), (2*R*,3*R*)-**8a** showed its potential as an orally active drug.

Uterine wet weight assay and morphometric analysis

The uterotrophic assay is a well-established method to measure the effect of a compound on uterine. As the induction of uterine cancer is a main side effect of tamoxifen, its estrogenicity of increasing uterine wet weight and luminal epithelial cell height (LECH) was detected by this method reported in previous studies. Fong et al. (2007) To investigate the stimulatory effect on uterine of (2*R*,3*R*)-**8a**, the uterotrophic assay was taken and uterine wet weight, luminal epithelial cell height, and luminal circumference were measured. An ovariectomized (OVX) mice model and 30 healthy female kunming mouse were randomly assigned to five groups: a sham operated group in which only a piece of fat around the ovary was ablated (SHAM) and four groups of OVX mouse, including the placebo (OVX+NS), the tamoxifen positive control (OVX+TAM), low dosage and high dosage (OVX+(2*R*,3*R*)-**8a**) group. Compared with the vehicle OVX+NS group, OVX+TAM group and SHAM group showed significant increase in all three indicators, while OVX+(2*R*,3*R*)-**8a** groups exhibited no stimulating effects on any aspects measured (Table 4 and Fig. 5), which indicated that (2*R*,3*R*)-**8a** may have beneficial compared with tamoxifen in overcoming the endometrial side effect.

Cell circle analysis and evaluation of apoptosis with flow cytometry

Further investigation of effects of (2*R*,3*R*)-**8a** on MCF-7 cell apoptosis and cell cycle suggested that it might induce MCF-7 cell apoptosis dose dependently and affect cell circle by arresting cells at G0/G1 phase at a concentration of 4.50 μM (Table 5). G0/G1 arrest caused by tamoxifen was also observed by other studies (Khamis et al. 2018). In Annexin V-FITC/PI dual staining assay, MCF-7 cells were treated with (2*R*,3*R*)-**8a** for 72 h at three different concentrations, respectively, to examine the apoptotic effect (Table 6). The results demonstrated that (2*R*,3*R*)-**8a**

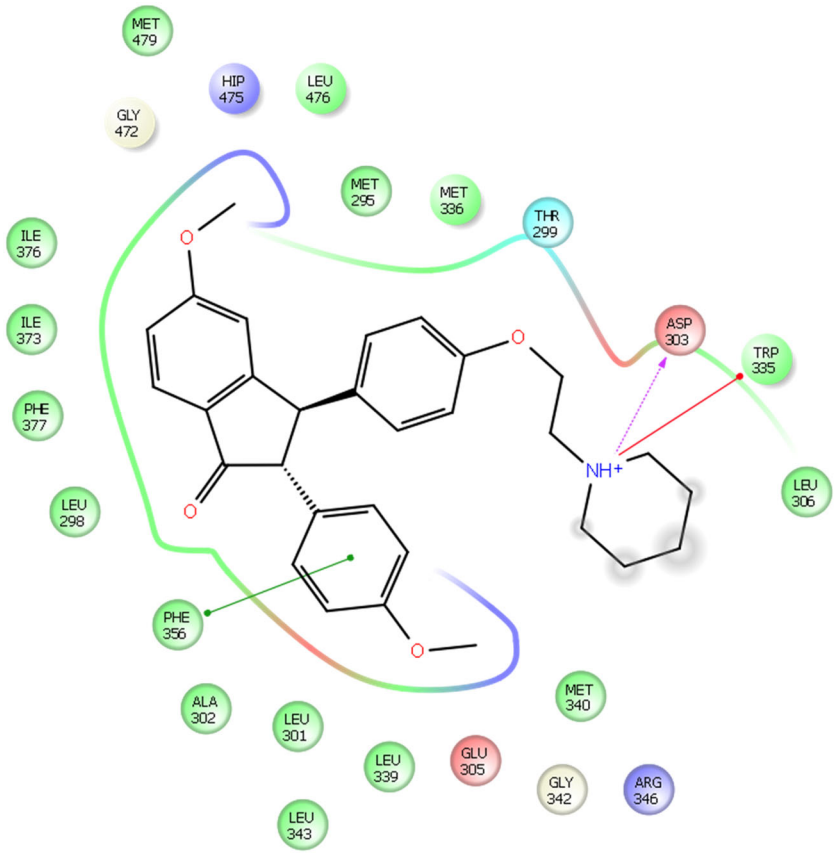

Fig. 4 Interactions between ERβ-binding pocket and (2*R*,3*R*)-**8a**;

Table 3 Results of radiometric competitive binding assay

Compound	ER-binding affinity % max (20 μM)		*β*/*α* ratio
	ERα	ERβ	
8a	42.48	170.97	4.02
8c	36.74	67.52	1.84
(2*R*,3*R*)-**8a**	30.10	210.33	6.98
(2*S*,3*S*)-**8a**	49.28	135.30	2.74

showed a trend to induce apoptosis against MCF-7 cells. It induced 44.7%, 59.0%, and 88.6% early and late apoptosis at 4.50, 6.00 and 7.50 μM concentrations, respectively, for 72 h. Although the cell cytostatic and cytotoxic capability of (2*R*,3*R*)-**8a** demonstrated similar patterns with tamoxifen, further studies on gene expression level are still needed to learn more about the detailed mechanism.

In vitro metabolic stability studies

As analog (2*R*,3*R*)-**8a** has performed noticeably in former studies, it was decided to conduct in vitro metabolic stability experiment with rat liver microsome, which is commonly used as candidate screening tool in the early stage of drug development. Analog (2*R*,3*R*)-**8a** was incubated with rat liver microsome at 37 °C for 1 h. The results showed that $T_{1/2}$ and CL_{int} of (2*R*,3*R*)-**8a** were 63 min and 0.022 mL/min/mg, whereas $T_{1/2}$ and CL_{int} of isopaucifloral F were > 145 min and < 0.001 mL/min/mg. The results indicated the metabolic stability of (2*R*,3*R*)-**8a** and contributed to its druggability. Shorter $T_{1/2}$ might be the influenced by the oxidation of its side chain substitute. Further in vivo study and analysis will be undertook to confirm the prediction and explore the metabolic pathways.

Materials and methods

Materials and physical measurements

Reagents were purchased from Aldrich, TCI, Shaoyuan and Energy Chemical companies. [2,4,6,7-^{3}H]-E2 (81.0 ci/mmol) was purchased from PerkinElmer Company. All solvents were purified and dried in accordance with standard procedures unless otherwise indicated. Oxygen-free and water-free operations were carried out under N_2 in dried glassware unless otherwise noted. Reactions were

Table 4 Effect of (2*R*,3*R*)-**8a** on uterine wet weight, luminal epithelial cell height (LECH), and luminal circumference

	Uterine wet weight (g)[a]	Luminal epithelial cell height (μm)[b]	Luminal circumference (mm)[b]
OVX+NS	0.06 ± 0.03	48.83 ± 5.95	0.69 ± 0.28
OVX+(2*R*,3*R*)-**8a**-low	0.05 ± 0.01	42.20 ± 11.00	1.09 ± 0.32
OVX+(2*R*,3*R*)-**8a**-high	0.06 ± 0.01	–	–
OVX+TAM	0.16 ± 0.04*	114.57 ± 2.65*	1.79 ± 0.57*
SHAM	0.17 ± 0.05*	77.07 ± 7.29*	2.85 ± 2.03*

OVX+NS ovariectomized mice with sesame oi, *OVX+TAM* ovariectomized mice with 0.1 mg/kg tamoxifen, *OVX+(2R,3R)-**8a**-low* ovariectomized mice with 0.1 mg/kg (2*R*,3*R*)-**8a**, *OVX+(2R,3R)-**8a**-high* ovariectomized mice with 1 mg/kg (2*R*,3*R*)-**8a**, *SHAM* sham-operated group

*$P < 0.05$ vs OVX+NS

[a]$n = 6$

[b]$n = 3$

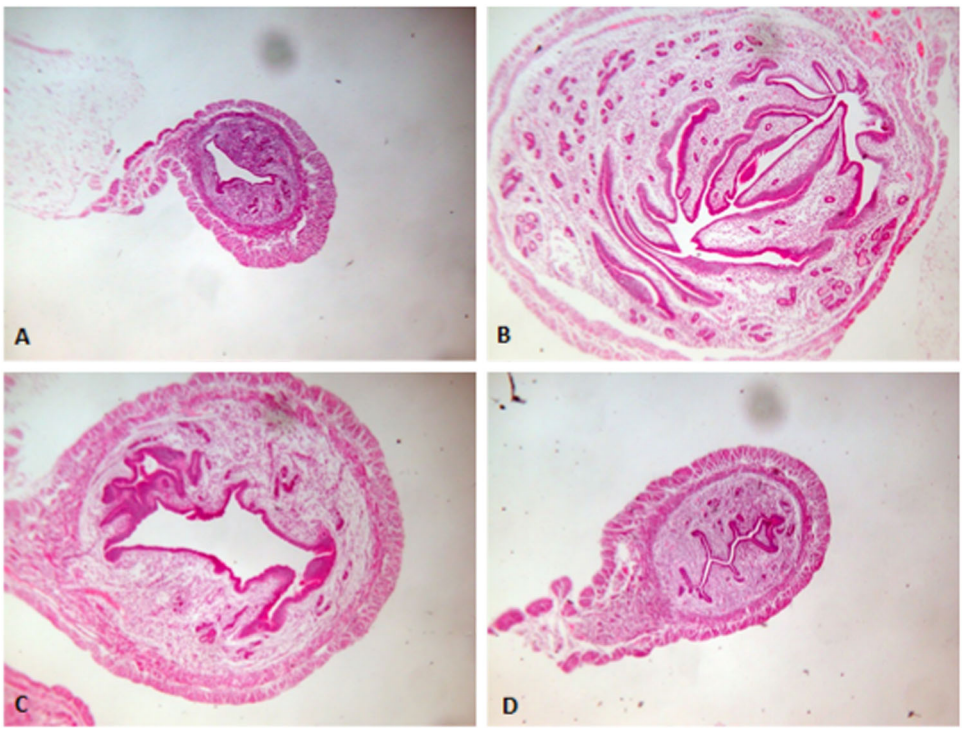

Fig. 5 Hematoxylin and eosin-stained sections of uterine tissue at × 100 magnification; after three daily doses of **a** OVX with sesame oil, **b** SHAM with sesame oil, **c** OVX with 100 μg/kg TAM, and **d** OVX with 100 μg/kg (2*R*,3*R*)-**8a**. TAM treatment and endogenous estrogen exposure (SHAM) induced increases in luminal epithelial cell height. Luminal circumference is increased to a greater degree by endogenous estrogen exposure than TAM

Table 5 Effect of different concentration of (2*R*,3*R*)-**8a** on cell circle of MCF-7 cell line after 24 h treatment

Concentration (μM)	apoptosis	G0/G1 phase	S phase
0	4.50%	53.65%	41.87%
4.50	27.81%	45.70%	26.48%
6.00	40.44%	31.65%	27.90%

monitored by thin-layer chromatography using Yantai (China) GF254 silica gel plates (5 × 10 cm). Silica gel column chromatography was performed on silica gel (300–400 mesh) from Yantai (China). All ^{1}H-NMR spectra were recorded on Varian Mercury 300 (300 MHz) or Bruker DRX-400 (400 MHz) spectrometers and ^{13}C-NMR spectral data were recorded on a Bruker DPX-400 (100 MHz) spectrometer. Low-resolution mass spectra (ESI) were obtained on a Shimadzu LCMS-2010EV and higher resolution mass spectra were obtained on an IonSpec 4.7 Tesla FTMS (MALDI) or a Bruker Daltonics, Inc. APEXIII7.0 TESLA FMS (ESI). Melting points (m.p.) were determined using an X-4 microscope melting point apparatus; Infrared radiation (IR) spectra were recorded on a Thermo Scientific Nicolet 380 FT-IR spectrometer. Optical rotations were measured on an Auto-pol V polarimeter.

Table 6 Effect of different concentration of (2*R*,3*R*)-**8a** on apoptosis of MCF-7 cell line after 72 h treatment

Concentration (μM)	Living cells	Early apoptotic cells	Late apoptotic cells	Apoptosis rate
0	59.2%	5.2%	35.4%	40.6%
4.50	54.3%	10.5%	34.2%	44.7%
6.00	40.5%	9.7%	49.3%	59.0%
7.50	7.1%	10.4%	78.2%	88.6%

Chemistry

(4-Methoxybenzyl)diphenylphosphine oxide (9)

In a 250 mL round-bottom flask, magnesium (3.00 g, 0.13 mol), trace of iodine, and anhydrous tetrahydrofuran (THF) (190 mL) were charged under N_2 at room temperature. A solution of *p*-MeO-PhCH_2Cl (19.58 g, 0.13 mol) in anhydrous THF (10 mL) was added dropwise to the reaction. Then the reaction was heated and refluxed for 4.5 h until magnesium was completely consumed. After the reaction mixture was cooled down in an ice bath, a mixture of Ph_2PCl (21.24 mL, 0.12 mmol) and anhydrous THF (10 mL) was added dropwise. Then the reaction mixture was heated to reflux overnight. The reaction mixture was cooled down and 30% H_2O_2 (20 mL) was added. After evaporated most of THF, the residue was extracted with CH_2Cl_2 (100 mL × 3). The combined organic layer was washed with saturated $NaHCO_3$, brine, dried with anhydrous Na_2SO_4 and concentrated. The obtained light yellow solid was washed subsequently with ethyl acetate and methanol to give **9** (28.07 g, 67%) as a white solid, mp: 233–235 °C; IR (film) 2927, 2849, 1666, 1540, 1426, 1310, 1311, 1120, 1046, 1015, 810, 503 cm^{-1}; ^{1}H-NMR ($CDCl_3$, 400 MHz) δ: 3.59 (d, J = 13.2 Hz, 2H), 3.74 (s, 3H), 6.73 (d, J = 8.8 Hz, 2H), 7.02 (d, J = 7.2 Hz, 2H), 7.43–7.71 (m, 10H); ^{13}C-NMR ($CDCl_3$, 75 MHz) δ: 36.7, 37.3, 55.2, 113.7, 113.9, 113.9, 122.8, 122.9, 128.4, 128.5, 131.1, 131.1, 131.1, 131.2, 131.8, 131.8, 132.8, 158.5, 158.5; MS *m/z*: 322 $(M)^+$

(4-Hydroxybenzyl)diphenylphosphine oxide (10)

To a solution of (4-methoxybenzyl)diphenylphosphine oxide (Dotzlaq 1997) (3.22 g, 10 mmol) in anhydrous CH_2Cl_2 (100 mL), BBr_3 (2.4 mL, 25 mmol) was added under N_2 at 0 °C. The reaction was stirred at room temperature for 8 h and then quenched with water. The mixture was extracted with ethyl acetate (100 mL) and the organic layer was washed with water, brine and dried with anhydrous Na_2SO_4. After evaporated the solvent, the obtained solid was washed with CH_2Cl_2 to give pure **10** (2.03 g, 66%) as white powder. mp: 177–178 °C; IR (film) 3354, 3005, 2934, 1716, 1688, 1433, 1423, 1334, 1266, 1056, 753 cm^{-1}; ^{1}H-NMR (400 MHz, CD_3OD) δ 3.73 (d, J = 13.1 Hz, 2H), 6.58 (d, J = 8.3 Hz, 2H), 6.82–6.99 (m, 2H), 7.41–7.83 (m, 10H); ESIMS *m/z*: 309.2 $(M+H)^+$.

(4-(2-(Benzyloxy)ethoxy)benzyl)diphenylphosphine oxide (11)

To a solution of (4-hydroxybenzyl)diphenylphosphine oxide (Fox et al. 2008) (3.08 g, 10 mmol) and 2-(benzyloxy)ethyl-4-methylbenzenesulfonate (3.06 g, 10 mmol) in anhydrous dimethylformamide (DMF), anhydrous cesium carbonate (13.03 g, 40 mmol), and tetrabutyl ammonium iodide (TBAI) (154 mg) were added. The reaction was stirred at 80 °C for 2 h and then quenched with water. The mixture was extracted with ethyl acetate (100 mL × 3) and the combined organic layer was washed with water, brine and dried with anhydrous Na_2SO_4. After evaporated the solvent, the obtained solid was washed with ethyl ether (30 mL) to give **11** (3.45 g, 78%) as white powder. mp: 221–222 °C; IR (film) 2917, 2822, 1709, 1623, 1514, 1477, 1354, 1347, 1266, 1078, 754 cm^{-1}; ^{1}H-NMR (400 MHz, $CDCl_3$) δ 3.61 (d, J = 13.5 Hz, 2H), 3.75–3.82 (m, 2H), 4.04–4.10 (m, 2H), 6.75 (d, J = 8.5 Hz, 2H), 7.00 (dd, J = 2.0, 8.6 Hz, 2H), 7.26–7.68 (m, 15H); ^{13}C-NMR (100 MHz, $CDCl_3$) δ 67.3, 68.4, 73.3, 114.6, 127.7, 127.8, 128.4, 128.5, 131.0, 131.1, 131.2, 131.7; ESIMS *m/z*: 443.0 $(M+H)^+$.

(4-(2-Hydroxyethoxy)benzyl)diphenylphosphine oxide (12)

To a solution of {4-[2-(benzyloxy)ethoxy]benzyl}diphenylphosphine oxide (Hartman et al. 2009) (4.42 g, 10 mmol) in anhydrous CH_2Cl_2 (100 mL), aluminum trichloride (2.00 g, 15 mmol) was added under ice bath. The reaction mixture was stirred at room temperature for 2 h, cooled to 0 °C, and quenched with water. After evaporated most of CH_2Cl_2, the solution was extracted with ethyl acetate (100 mL × 3). The combined organic layer was washed with water, brine and dried with anhydrous Na_2SO_4. After evaporated the solvent, the obtained solid was further washed with ethyl ether to give **12** (3.45 g, 98%) as white powder. mp: 137–138 °C; IR (film) 3324, 3010, 2925, 2873, 1737, 1639, 1482, 1354, 1337, 1206, 1162, 1067, 1023, 853 cm^{-1}; ^{1}H-NMR (400 MHz, $CDCl_3$) δ 3.59 (d, J = 13.3 Hz, 2H),

3.90–3.92 (m, 2H), 3.99–4.01 (m, 2H), 6.73 (d, $J = 8.4$ Hz, 2H), 7.01 (d, $J = 8.3$ Hz, 2H), 7.41–7.70 (m, 10H); ESIMS *m/z*: 353.2 $(M+H)^+$.

2-(4-((Diphenylphosphoryl)methyl)phenoxy)ethyl-4-methylbenzenesulfonate (13)

To a solution of [4-(2-hydroxyethoxy)benzyl]diphenylphosphine oxide (Ström et al. 2004) (3.52 g, 10 mmol) in anhydrous CH_2Cl_2 (100 mL), triethylamine (50 mL) and paratoluensulfonyl chloride (1.99 g, 10.5 mmol) were added. The resulting mixture was heated to 50 °C for 20 h and then quenched with water. The mixture was extracted with CH_2Cl_2 (100 mL × 3) and the combined organic layer was washed with water, brine and dried with anhydrous Na_2SO_4. After evaporated the solvent, the obtained solid was further washed with ethyl ether to give **13** (3.09 g, 61%) as white powder. mp: 245–246 °C; IR (film) 2919, 1742, 1634, 1489, 1356, 1321, 1211, 1150, 1121, 1029, 1011, 850, 520 cm^{-1}; ^{1}H-NMR (400 MHz, $CDCl_3$) δ 2.44 (s, 3H), 3.58 (d, $J = 13.3$ Hz, 2H), 4.03–4.11 (m, 2H), 4.26–4.36 (m, 2H), 6.60 (d, $J = 8.4$ Hz, 2H), 6.99 (d, $J = 6.8$ Hz, 2H), 7.26–7.81 (m, 14H).

General procedure for the syntheses of (4-(2-(naphthenic amino)ethoxy)- benzyl)diphenylphosphine oxide (14a–g)

To a solution of 2-{4-[(diphenylphosphoryl)methyl]phenoxy} ethyl-4-methylbenzenesulfonate (Mak et al. 2006) (1.00 mmol) and naphthenic amino (1.00 mmol) in anhydrous DMF (anhydrous cesium carbonate (4.00 mmol) and TBAI (25 mg) were added. The reaction was stirred at 80 °C for 2 h and quenched with water. The mixture was extracted with ethyl acetate (100 mL × 3) and the combined organic layer was washed with water, brine and dried with anhydrous Na_2SO_4. After evaporated the solvent, the obtained solid was washed with ethyl ether (20 mL) to give **14a–g** as white powder.

Diphenyl(4-(2-(piperidin-1-yl)ethoxy)benzyl)phosphine oxide (14a) White solid, yield 79%. mp: 199–200 °C; IR (film) 2920, 2850, 1699, 1620, 1413, 1401, 1358, 1308, 1271, 1201, 1147, 1020 cm^{-1}; ^{1}H-NMR (400 MHz, $CDCl_3$) δ 1.46 (s, 2H), 1.63 (s, 4H), 2.53 (s, 4H), 2.78 (s, 2H), 3.58 (d, $J = 13.3$ Hz, 2H), 4.07 (s, 2H), 6.72 (d, $J = 8.4$ Hz, 2H), 7.00 (d, $J = 7.3$ Hz, 2H), 7.26–7.71 (m, 10H); ^{13}C-NMR (100 MHz, $CDCl_3$) δ 23.9, 25.6, 36.7, 37.4, 54.9, 57.7, 114.5, 128.4, 128.5, 131.0, 131.2, 131.7, 131.7, 131.8, 132.8; ESIMS *m/z*: 420.2 $(M+H)^+$.

Diphenyl(4-(2-(pyrrolidin-1-yl)ethoxy)benzyl)phosphine oxide (14b) White solid, yield 73%. mp: 189–190 °C; IR (film) 2923, 2855, 1734, 1619, 1517, 1428, 1300, 1222, 1143, 1110, 1037, 826 cm^{-1}; ^{1}H-NMR (400 MHz, $CDCl_3$) δ 1.82 (s, 4H), 2.64 (s, 4H), 2.89 (t, $J = 5.8$ Hz, 2H), 3.61 (d, $J = 13.3$ Hz, 2H), 4.06 (t, $J = 5.9$ Hz, 2H), 6.76 (d, $J = 8.2$ Hz, 2H), 7.02 (d, $J = 8.0$ Hz, 2H), 7.44–7.73 (m, 10H); ^{13}C-NMR (100 MHz, $CDCl_3$) δ 23.4, 36.8, 37.4, 54.7, 55.0, 66.8, 114.5, 123.0, 128.4, 128.5, 131.0, 131.1, 131.2, 131.7, 131.8, 132.9, 157.7; ESIMS *m/z*: 406.2 $(M+H)^+$.

Diphenyl(4-(2-(2-methylpiperidin-1-yl)ethoxy)benzyl)phosphine oxide (14c) White solid, yield 71%. mp: 168–169 °C; IR (film) 2930, 1724, 1620, 1499, 1357, 1314, 1206, 1142, 1133 1009 cm^{-1}; ^{1}H-NMR (400 MHz, $CDCl_3$) δ 1.12 (d, $J = 5.4$ Hz, 3H), 1.31 (s, 2H), 1.60 (s, 4H), 2.35 (s, 2H), 2.80 (s, 1H), 2.94 (d, $J = 9.9$ Hz, 1H), 3.07 (d, $J = 6.5$ Hz, 1H), 3.59 (d, $J = 13.3$ Hz, 2H), 4.02 (s, 2H), 6.72 (d, $J = 8.4$ Hz, 2H), 7.00 (d, $J = 8.3$ Hz, 2H), 7.43–7.71 (m, 10H); ^{13}C-NMR (100 MHz, $CDCl_3$) δ 23.8, 25.8, 34.3, 36.7, 37.4, 52.5, 53.3, 56.4, 65.3, 114.4, 114.4, 122.9, 123.0, 128.4, 128.5, 131.0, 131.1, 131.2, 131.7, 131.7, 131.8, 132.8, 157.6; ESIMS *m/z*: 434.2 $(M+H)^+$.

Diphenyl(4-(2-(4-methylpiperidin-1-yl)ethoxy)benzyl) phosphine oxide (14d) White solid, yield 81%. mp: 178–179 °C; IR (film) 2929, 1734, 1656, 1483, 1337, 1332, 1223, 1145, 1057 cm^{-1}; ^{1}H-NMR (400 MHz, $CDCl_3$) δ 0.92 (d, $J = 6.1$ Hz, 3H), 1.17–1.41 (m, 3H), 1.62 (d, $J = 11.8$ Hz, 2H), 1.98–2.14 (m, 2H), 2.75 (s, 2H), 2.94 (d, $J = 10.3$ Hz, 2H), 3.59 (d, $J = 13.3$ Hz, 2H), 4.04 (t, $J = 5.8$ Hz, 2H), 6.73 (d, $J = 8.4$ Hz, 2H), 7.00 (d, $J = 6.8$ Hz, 2H), 7.29–7.80 (m, 10H); ^{13}C-NMR (100 MHz, $CDCl_3$) δ 21.8, 30.5, 34.1, 36.8, 37.4, 54.5, 57.5, 65.9, 114.5, 123.0, 128.4, 128.5, 131.0, 131.1, 131.1, 131.2, 131.7, 131.9, 132.8, 157.7; ESIMS *m/z*: 434.2 $(M+H)^+$.

Diphenyl(4-(2-(4-cyclohexylpiperazin-1-yl)ethoxy)benzyl) phosphine oxide (14e) White solid, yield 67%. mp: 199–200 °C; IR (film) 2933, 1754, 1657, 1466, 1369, 1329, 1310, 1140, 1029 cm^{-1}; ^{1}H-NMR (400 MHz, $CDCl_3$) δ 0.99–1.30 (m, 6H), 1.61 (d, $J = 11.5$ Hz, 1H), 1.77 (s, 2H), 1.88 (d, $J = 8.3$ Hz, 2H), 2.23 (s, 1H), 2.30 (s, 1H), 2.61 (s, 6H), 2.76 (t, $J = 5.7$ Hz, 2H), 3.57 (d, $J = 13.3$ Hz, 2H), 4.01 (dd, $J = 8.2$, 13.9 Hz, 2H), 6.71 (d, $J = 7.6$ Hz, 2H), 6.99 (d, $J = 8.4$ Hz, 2H), 7.33–7.80 (m, 10H); ^{13}C-NMR (100 MHz, $CDCl_3$) δ 25.8, 26.2, 28.9, 36.7, 37.4, 45.9, 48.8, 54.0, 57.2, 63.5, 65.7, 76.7, 77.0, 77.3, 114.5, 114.5, 122.9, 123.0, 128.4, 128.5, 131.0, 131.1, 131.2, 131.7, 131.7, 131.8, 132.8, 157.7; ESIMS *m/z*: 503.2 $(M+H)^+$.

(4-(2-Morpholinoethoxy)benzyl)diphenylphosphine oxide (14f) White solid, yield 52%. mp: 179–180 °C; IR (film) 2936, 1778, 1623, 1456, 1479, 1338, 1320, 1231, 1204, 1153, 1119, 1045, 1067, 836 cm^{-1}; ^{1}H-NMR (400 MHz, $CDCl_3$) δ 2.50 (t, $J = 4.3$ Hz, 4H), 2.69–2.72 (m, 2H), 3.54 (d, $J = 13.3$ Hz, 2H), 3.67 (t, $J = 4.7$ Hz, 4H), 3.97–4.00

(m, 2H), 6.68 (d, $J = 8.6$ Hz, 2H), 6.96–6.98 (m, 2H), 7.35–7.67 (m, 10H); ESIMS *m/z*: 422.0 $(M+H)^+$.

(4-(2-(3,4-Dihydroisoquinolin-2(1H)-yl)ethoxy)benzyl) diphenylphosphine oxide (14g) White solid, yield 52%. mp: 177–178 °C; IR (film) 2945, 2811, 1725, 1613, 1517, 1456, 1348, 1210, 1214, 1130, 1028, 811 cm^{-1}; ^{1}H-NMR (400 MHz, $CDCl_3$) δ2.87−2.97 (m, 6H), 3.59 (d, $J =$ 13.2 Hz, 2H), 3.77 (s, 2H), 4.14 (t, $J = 5.6$ Hz, 2H), 6.76 (d, $J = 8.4$ Hz, 2H), 7.01 (dd, $J = 8.4$ Hz, $J = 2$ Hz, 3H), 7.08–7.13 (m, 3H), 7.41–7.52 (m, 6H), 7.66–7.71 (m, 4H); ESIMS *m/z*: 468.0 $(M+H)^+$.

General procedure for the synthesis of 1,2-bis(3,5-dimethoxyphenyl)-3-(4- (2-(aminoalkyl-1-yl)ethoxy) phenyl) prop-2-en-1-ones (17a–f) and 1,2-bis(4-methoxy-phenyl)-3-(4-(2-(aminoalkyl-1-yl)ethoxy) phenyl)prop-2-en-1-ones (18a–f)

To a solution of oxybenzoic acid substituted by methyl (**15** or **16**) (3.02 mmol) and diphenyl{4-[2-(aminoalkyl-1-yl) ethoxy]benzyl}phosphine oxide (3.02 mmol) in anhydrous toluene (100 mL), NaHMDS (2 M, 6.05 mmol) in THF was added under N_2 at room temperature. The reaction mixture was quenched with water after 0.5 h stirring. The reaction mixture was concentrated and then diluted with ethyl acetate. The organic layer was washed with water (30 mL) and brine (30 mL), dried over Na_2SO_4, filtered, and evaporated. The obtained residue was further purified by silica gel column chromatography (0–10% ethyl acetate/hexanes) to give the desired product as yellowish oil.

1,2-Bis(3,5-dimethoxyphenyl)-3-(4-(2-(piperidin-1-yl) ethoxy)phenyl)prop-2-en-1-one (17a) Yellowish oil, yield 67%. IR (film) 2932, 1722, 1637, 1449, 1433, 1418, 1314, 1204, 1130, 1026 cm^{-1}; ^{1}H-NMR (400 MHz, $CDCl_3$) δ 1.43 (d, $J = 4.7$ Hz, 2H), 1.59 (dt, $J = 5.4$, 10.8 Hz, 4H), 2.48 (s, 4H), 2.72 (t, $J = 5.9$ Hz, 2H), 3.75 (s, 6H), 3.76 (s, 6H), 4.04 (t, $J = 6.0$ Hz, 2H), 6.36–6.75 (m, 6H), 7.06–7.28 (m, 5H); ESIMS *m/z*: 532.2 $(M+H)^+$.

1,2-Bis(3,5-dimethoxyphenyl)-3-(4-(2-(pyrrolidin-1-yl) ethoxy)phenyl)prop-2-en-1-one (17b) Yellowish oil, yield 65%. IR (film) 2917, 1707, 1602, 1477, 1439, 1355, 1306, 1223, 1203, 1141, 1027, 900 cm^{-1}; ^{1}H-NMR (400 MHz, $CDCl_3$) δ 1.82 (d, $J = 2.9$ Hz, 4H), 2.62 (s, 4H), 2.88 (t, $J =$ 6.0 Hz, 2H), 3.66–3.89 (m, 12H), 4.06 (t, $J = 5.9$ Hz, 2H), 6.41–6.78 (m, 6H), 7.11–7.28 (m, 5H); ESIMS *m/z*: 518.2 $(M+H)^+$.

1,2-Bis(3,5-dimethoxyphenyl)-3-(4-(2-(2-methylpiperidin-1-yl)ethoxy)-phenyl)prop-2-en-1-one (17c) Yellowish oil, yield 70%. IR (film) 2946, 2845, 1701, 1633, 1576, 1473, 1446, 1348, 1288, 1214, 1154, 1140, 1028, 732 cm^{-1}; ^{1}H-NMR (400 MHz, $CDCl_3$) δ 1.11 (t, $J = 8.7$ Hz, 3H), 1.25–1.35 (m, 2H), 1.61 (ddd, $J = 7.1$, 16.0, 33.7 Hz, 4H), 2.27–2.41 (m, 2H), 2.70–2.80 (m, 1H), 2.92 (d, $J =$ 11.4 Hz, 1H), 3.00–3.13 (m, 1H), 3.57–3.90 (m, 12H), 3.95–4.06 (m, 2H), 6.40–6.75 (m, 6H), 7.10–7.22 (5H, m); ESIMS *m/z*: 546.2 $(M+H)^+$.

1,2-Bis(3,5-dimethoxyphenyl)-3-(4-(2-(4-methylpiperidin-1-yl)ethoxy)-phenyl)prop-2-en-1-one (17d) Yellowish oil, yield 72%. IR (film) 2940, 1715, 1624, 1496, 1427, 1367, 1306, 1211, 1148, 1021 cm^{-1}; ^{1}H-NMR (400 MHz, $CDCl_3$) δ 0.92 (d, $J = 6.1$ Hz, 3H), 1.24–1.31 (m, 3H), 1.62 (d, $J =$ 12.3 Hz, 2H), 2.07 (t, $J = 10.8$ Hz, 2H), 2.74 (t, $J = 6.0$ Hz, 2H), 2.93 (d, $J = 11.5$ Hz, 2H), 3.76 (s, 6H), 3.77 (s, 6H), 4.04 (t, $J = 6.0$ Hz, 2H), 6.40–6.75 (m, 6H), 7.10–7.22 (m, 5H); ESIMS *m/z*: 546.2 $(M+H)^+$.

3-(4-(2-(4-Cyclohexylpiperazin-1-yl)ethoxy)phenyl)-1,2-bis (3,5-dimethoxy-phenyl)prop-2-en-1-one (17e) Yellowish oil, yield 52%. IR (film) 2935, 1734, 1611, 1426, 1445, 1356, 1326, 1211, 1037, 555, 460 cm^{-1}; ^{1}H-NMR (400 MHz, $CDCl_3$) δ 1.07–1.30 (m, 6H), 1.58–2.21 (m, 7H), 2.58 (s, 6H), 2.73 (s, 2H), 3.73 (s, 6H), 4.00 (s, 2H), 6.36–6.71 (m, 6H), 6.92–7.22 (m, 5H); ESIMS *m/z*: 515.0 $(M+H)^+$.

1,2-Bis(3,5-dimethoxyphenyl)-3-(4-(2-morpholinoethoxy) phenyl)prop-2-en-1-one (17f) Yellowish oil, yield 57%. IR (film) 2923, 2850, 1708, 1627, 1532, 1486, 1456, 1420, 1322, 1310, 1226, 1205, 1150, 1018, 670, 452 cm^{-1}; ^{1}H-NMR (400 MHz, $CDCl_3$) δ 2.55 (s, 4H), 2.74–2.77 (m, 2H), 3.70–3.73 (m, 4H), 3.75 (s, 6H), 3.76 (s, 6H), 4.03–4.06 (m, 2H), 6.39–6.74 (m, 6H), 7.08–7.21 (m, 5H); ESIMS *m/z*: 534.0 $(M+H)^+$.

1,2-Bis(4-methoxyphenyl)-3-(4-(2-(piperidin-1-yl)ethoxy) phenyl)prop-2-en-1-one (18a) Yellowish oil, yield 57%. IR (film) 2921, 2828, 1711, 1632, 1590, 1411, 1425, 1312, 1316, 1218, 1205, 1137, 1056, 1047, 788, 641 cm^{-1}; ^{1}H-NMR (400 MHz, $CDCl_3$) δ 1.43 (d, $J = 5.1$ Hz, 2H), 1.55–1.61 (m, 4H), 2.47 (s, 4H), 2.72 (t, $J = 6.1$ Hz, 2H), 3.78 (s, 3H), 3.80 (s, 3H), 4.02 (t, $J = 6.0$ Hz, 2H), 6.70 (d, $J = 8.6$ Hz, 2H), 6.82–6.86 (m, 4H), 7.00 (s, 1H), 7.20 (d, $J = 8.6$ Hz, 2H), 7.36 (d, $J = 9.0$ Hz, 2H), 7.97 (d, $J =$ 8.6 Hz, 2H); ESIMS *m/z*: 472.0 $(M+H)^+$.

1,2-Bis(4-methoxyphenyl)-3-(4-(2-(4-methylpiperidin-1-yl) ethoxy)phenyl)-prop-2-en-1-one (18b) Yellowish oil, yield 56%. IR (film) 2942, 2834, 1633, 1622, 1567, 1456, 1422, 1297, 1250, 1233, 1071, 1038, 763, 554 cm^{-1}; ^{1}H-NMR

(400 MHz, ($CDCl_3$) δ 1.25–1.34 (m, 6H), 1.60 (d, J = 11.2 Hz, 2H), 2.08 (t, J = 11.6 Hz, 2H), 2.75 (t, J = 11.6 Hz, 2H), 2.94 (d, J = 11.6 Hz, 2H), 3.76 (s, 3H), 3.77 (s, 3H), 4.03 (t, J = 6.0 Hz, 2H), 6.69 (d, J = 8.8 Hz, 2H), 6.82 (t, J = 8.8 Hz, 4H), 6.99 (s, 1H), 7.19 (d, J = 8.8 Hz, 2H), 7.35 (d, J = 8.8 Hz, 2H), 7.96 (d, J = 8.8 Hz, 2H); ESIMS *m/z*: 486.0 $(M+H)^+$.

1,2-Bis(4-methoxyphenyl)-3-(4-(2-morpholinoethoxy)phenyl)prop-2-en-1-one (18c) Yellowish oil, yield 52%. IR (film) 2934, 2847, 1612, 1500, 1433, 1456, 1245, 1240, 1075, 1026, 860, 542 cm^{-1}; ^{1}H-NMR (400 MHz, $CDCl_3$) δ 2.56 (m, 4H), 2.76 (t, J = 5.6 Hz, 2H), 3.72 (t, J = 4.8 Hz, 4H), 3.78 (s, 3H), 3.80 (s, 3H), 4.04 (t, J = 5.6 Hz, 2H), 6.70 (d, J = 8.8 Hz, 2H), 6.84 (t, J = 8.8 Hz, 4H), 7.00 (s, 1H), 7.21 (d, J = 8.8 Hz, 2H), 7.36 (d, J = 8.8 Hz, 2H), 7.97 (d, J = 8.8 Hz, 2H); ESIMS *m/z*: 474.0 $(M+H)^+$.

1,2-Bis(4-methoxyphenyl)-3-(4-(2-(4-cyclohexylpiperazin-1-yl)ethoxy)-phenyl)prop-2-en-1-one (18d) Yellowish oil, yield 52%. IR (film) 2926, 1693, 1576, 1478, 1447, 1411, 1354, 1301, 1242, 1211, 1104, 1029, 668, 560 cm^{-1}; ^{1}H-NMR (400 MHz, $CDCl_3$) δ 2.56 (m, 4H), 2.76 (t, J = 5.6 Hz, 2H), 3.72 (t, J = 4.8 Hz, 4H), 3.78 (s, 3H), 3.80 (s, 3H), 4.04 (t, J = 5.6 Hz, 2H), 6.70 (d, J = 8.8 Hz, 2H), 6.84 (t, J = 8.8 Hz, 4H), 7.00 (s, 1H), 7.21 (d, J = 8.8 Hz, 2H), 7.36 (d, J = 8.8 Hz, 2H), 7.97 (d, J = 8.8 Hz, 2H); ESIMS *m/z*: 555.1 $(M+H)^+$.

3-(4-(2-(3,4-Dihydroisoquinolin-2(1H)-yl)ethoxy)phenyl)-1,2-bis(4-methoxyphenyl)prop-2-en-1-one (18e) Yellowish oil, yield 43%. IR (film) 3000, 2912, 1686, 1581, 1489, 1478, 1429, 1310, 1244, 1211, 1037, 1026, 876, 563 cm^{-1}; ^{1}H-NMR (400 MHz, $CDCl_3$) δ 3.85–3.96 (m, 6H), 4.76 (s, 2H), 4.86 (s, 3H), 4.89 (s, 3H), 5.22 (t, J = 6.0 Hz, 2H), 7.89 (d, J = 8.8 Hz, 2H), 7.99–8.03 (m, 4H), 8.12–8.17 (m, 4H), 8.19 (s, 1H), 8.37 (d, J = 8.4 Hz, 2H), 8.49 (d, J = 8.8 Hz, 2H), 9.03 (d, J = 8.8 Hz, 2H); ESIMS *m/z*: 520.0 $(M+H)^+$.

1,2-Bis(4-methoxyphenyl)-3-(4-(2-(pyrrolidin-1-yl)ethoxy)phenyl)prop-2-en-1-one (18f) Yellowish oil, yield 49%. IR (film) 2923, 1755, 1724, 1627, 1517, 1480, 1454, 1427, 1329, 1216, 1228, 1148, 1023, 668, 573 cm^{-1}; ^{1}H-NMR (400 MHz, $CDCl_3$) δ 1.79 (m, 4H), 2.59 (m, 4H), 2.85 (t, J = 6 Hz, 2H), 3.79 (s, 3H), 3.81 (s, 3H), 4.03 (t, J = 6.0 Hz, 2H), 6.72 (d, J = 8.4 Hz, 2H), 6.84 (t, J = 8.4 Hz, 4H), 7.00 (s, 1H), 7.20 (d, J = 8.4 Hz, 2H), 7.36 (d, J = 8.4 Hz, 2H), 7.97 (d, J = 8.4 Hz, 2H); ESIMS *m/z*: 458.0 $(M+H)^+$.

General procedure for the synthesis of 2-(3,5-dihydroxyphenyl)-4,6-dihydroxy-3-(4-(2-(aminoalkyl-1-yl)ethoxy)phenyl)-2,3-dihydro-1H-inden-1-ones (5a–f) and 5-hydroxy-2-(4-hydroxyphenyl)-3-(4-(2-(aminoalkyl -1-yl)ethoxy)phenyl)-2,3-dihydro-1H-inden-1-ones (7a–d)

To an ice-cold solution of **17a–f** or **18a** or **18c** or **18e–f** (0.1 mmol) in CH_2Cl_2 (12 mL), $BBr_3{\cdot}OEt_2$ (1.5 mmol) was dropwise added via syringe. After stirred at room temperature for 8 h under N_2, the reaction was quenched with water (1–2 mL). After CH_2Cl_2 was evaporated, the saturated sodium bicarbonate solution was added to the mixture. The resulting solution was extracted with ethyl acetate (50 mL × 2) and the combined organic phase was washed with brine, dried over Na_2SO_4 and evaporated. The residue was further purified by silica gel column chromatography eluting with CH_3CN/H_2O/TFA (1: 2: 0.1%) to give the desired product as brown solid.

2-(3,5-Dihydroxyphenyl)-4,6-dihydroxy-3-(4-(2-(piperidin-1-yl)ethoxy)-phenyl)-2,3-dihydro-1H-inden-1-one (5a) Brown solid, yield 43%. mp: 233–234 °C; IR (film) 3345, 2923, 1760, 1633, 1450, 1432, 1417, 1355, 1325, 1234, 1154, 1076, 1022, 752, 521 cm^{-1};^{1}H-NMR (400 MHz, CD_3OD) δ 1.45–1.57 (m, 1H), 1.80 (t, J = 11.3 Hz, 3H), 1.93 (d, J = 11.9 Hz, 2H), 3.02 (t, J = 11.6 Hz, 2H), 3.36 (d, J = 2.5 Hz, 1H), 3.48–3.54 (m, 2H), 3.59 (d, J = 11.9 Hz, 2H), 4.25–4.36 (m, 2H), 4.43 (d, J = 2.2 Hz, 1H), 5.98 (d, J = 1.7 Hz, 2H), 6.16 (s, 1H), 6.64 (dd, J = 1.7, 30.1 Hz, 2H), 6.93 (dd, J = 8.5, 30.6 Hz, 4H); ^{13}C-NMR (100 MHz, CD_3OD) δ 22.5, 24.0, 52.3, 54.8, 57.1, 63.0, 67.0, 100.6, 102.3, 107.2, 110.9, 115.7, 129.3, 136.2, 138.5, 140.0, 143.1, 157.2, 157.7, 159.9, 160.9, 208.4; ESIMS *m/z*: 476.2 $(M+H)^+$; $C_{28}H_{30}NO_6$: HRMS calcd. 476.2068 $(M+H)^+$, found 476.2064.

2-(3,5-Dihydroxyphenyl)-4,6-dihydroxy-3-(4-(2-(pyrrolidin-1-yl)ethoxy)-phenyl)-2,3-dihydro-1H-inden-1-one (5b) Brown solid, yield 47%. mp: 205–206 °C; IR (film) 3356, 2941, 2824, 1711, 1632, 1486, 1442, 1400, 1324, 1300, 1221, 1151, 1023, 1050, 1012, 840, 811, 741, 502 cm^{-1}; ^{1}H-NMR (400 MHz, CD_3OD) δ 1.98–2.02 (m, 4H), 3,11–3.16 (m, 2H), 3.34 (d, J = 2.35 Hz, 1H), 3.56–3.59 (m, 2H), 3.67 (s, 2H), 4.24 (t, J = 4.7 Hz, 2H), 4.41 (d, J = 2.7 Hz, 1H), 5.97 (d, J = 2.0 Hz, 2H), 6.14 (t, J = 2.0 Hz, 1H), 6.59 (d, J = 2.3 Hz, 1H), 6.66 (d, J = 2.3 Hz, 1H), 6.88 (d, J = 8.6 Hz, 2H), 6.95 (d, J = 8.6 Hz, 2H); ^{13}C-NMR (100 MHz, CD_3OD) δ 21.0, 23.9, 52.3, 55.2, 55.7, 64.3, 67.0, 100.6, 102.4, 107.3, 111.0, 115.8, 129.4, 136.3, 138.6, 140.1, 143.1, 157.3, 157.8, 159.9, 160.0, 161.0, 208.5; ESIMS *m/z*: 462.2 $(M+H)^+$; $C_{27}H_{28}NO_6$: HRMS calcd. 462.1911 $(M+H)^+$, found 462.1911.

2-(3,5-Dihydroxyphenyl)-4,6-dihydroxy-3-(4-(2-morpholinoethoxy)phenyl)-2,3-dihydro-1H-inden-1-one (5c) Brown solid, yield 42%. mp: 217–219 °C; IR (film) 3356, 2916,

1734, 1622, 1478, 1429, 1433, 1353, 1300, 1214, 1167, 1123, 1036, 666, 453 cm^{-1}; ^{1}H-NMR (400 MHz, CD_3OD) δ 3.26 (m, 2H), 3.35 (d, $J = 2.7$ Hz, 1H), 3.55 (m, 2H), 3.60 (t, $J = 4.7$ Hz, 2H), 3.80 (m, 2H), 4.03 (m, 2H), 4.33–4.35 (m, 2H), 4.43 (d, $J = 2.4$ Hz, 1H), 5.98 (d, $J = 2.0$ Hz, 2H), 6.15 (t, $J = 2.0$ Hz, 1H), 6.60 (d, $J = 1.6$ Hz, 1H), 6.68 (d, $J = 2.0$ Hz, 1H), 6.92 (d, $J = 8.6$ Hz, 2H), 6.98 (d, $J = 8.6$ Hz, 2H); ^{13}C-NMR (100 MHz, CD_3OD) δ 52.3, 53.6, 57.5, 62.8, 64.9, 67.1, 100.6, 102.4, 107.3, 111.0, 115.8, 129.4, 136.3, 138.7, 140.1, 143.1, 157.3, 157.7, 160.0, 161.0, 208.5; ESIMS *m/z*: 478.0 $(M+H)^+$; $C_{27}H_{28}NO_7$: HRMS calcd. 478.1860 $(M+H)^+$, found 478.1862.

2-(3,5-Dihydroxyphenyl)-4,6-dihydroxy-3-(4-(2-(4-methylpiperidin-1-yl)-ethoxy)phenyl)-2,3-dihydro-1H-inden-1-one (5d) Brown solid, yield 60%. mp: 221–222 °C; IR (film) 3337, 2918, 2833, 1754, 1629, 1487, 1434, 1352, 1323, 1215, 1142, 1032, 754, 632 cm^{-1}; ^{1}H-NMR (400 MHz, CD_3OD) δ 0.99 (d, $J = 6.7$ Hz, 3H), 1.41–1.91 (m, 5H), 2.98–3.04 (m, 2H), 3.36 (d, $J = 2.7$ Hz, 1H), 3.49 (t, $J = 4.7$ Hz, 2H), 3.60 (d, $J = 12.5$ Hz, 2H), 4.29 (t, $J = 4.7$ Hz, 2H), 4.42 (d, $J = 2.7$ Hz, 1H), 5.98 (d, $J = 2.3$ Hz, 2H), 6.15–6.16 (m, 1H), 6.61 (d, $J = 2.3$ Hz, 1H), 6.68 (d, $J = 2.0$ Hz, 1H), 6.88 (d, $J = 8.6$ Hz, 2H), 6.96 (d, $J = 8.6$ Hz, 2H); ^{13}C-NMR (100 MHz, CD_3OD) δ 21.4, 29.7, 32.4, 52.3, 54.7, 57.3, 63.0, 67.0, 100.6, 102.3, 107.2, 111.0, 115.7, 129.3, 136.3, 138.5, 140.0, 143.1, 143.2, 157.3, 157.7, 159.9, 159.9, 160.9, 208.5; ESIMS *m/z*: 490.2 $(M+H)^+$; $C_{29}H_{32}NO_6$: HRMS calcd. 490.2224 $(M+H)^+$, found 490.2223.

2-(3,5-Dihydroxyphenyl)-4,6-dihydroxy-3-(4-(2-(2-methylpiperidin-1-yl)-ethoxy)phenyl)-2,3-dihydro-1H-inden-1-one (5e) Brown solid, yield 51%. mp: 251–252 °C; IR (film) 3356, 2924, 1736, 1622, 1478, 1436, 1329, 1320, 1210, 1142, 789, 531 cm^{-1}; ^{1}H-NMR (400 MHz, CD_3OD) δ 1.44 (d, $J = 5.9$ Hz, 3H), 1.54–2.00 (m, 6H), 3.03–3.09 (m, 1H), 3.36 (d, $J = 2.7$ Hz, 1H), 3.38–4.34 (m, 6H), 4.42 (d, $J = 2.7$ Hz, 1H), 5.99 (d, $J = 2.0$ Hz, 2H), 6.15–6.16 (m, 1H), 6.61 (d, $J = 2.3$ Hz, 1H), 6.68 (d, $J = 2.0$ Hz, 1H), 6.89 (d, $J = 8.6$ Hz, 2H), 6.97 (d, $J = 8.6$ Hz, 2H); ^{13}C-NMR (100 MHz, CD_3OD) δ 18.3, 22.9, 24.3, 30.7, 32.8, 52.3, 53.7, 54.2, 62.2, 63.0, 67.0, 100.6, 102.3, 107.2, 111.0, 115.7, 129.3, 136.3, 138.5, 140.0, 143.2, 157.3, 157.7, 159.9, 160.9, 208.5; ESIMS *m/z*: 490.0 $(M+H)^+$; $C_{29}H_{32}NO_6$: HRMS calcd. 490.2224 $(M+H)^+$, found 490.2221.

3-(4-(2-(4-Cyclohexylpiperazin-1-yl)ethoxy)phenyl)-2-(3,5-dihydroxy-phenyl)-4,6-dihydroxy-2,3-dihydro-1H-inden-1-one (5f) Brown solid, yield 42%. mp: 233–234 °C; IR (film) 3334, 2959, 1711, 1622, 1437, 1422, 1351, 1319, 1205, 1148, 1050, 1022, 757, 632 cm^{-1}; ^{1}H-NMR (400 MHz, CD_3OD) δ 1.17 (m, 6H), 1.69 (d, $J = 12.9$ Hz, 1H), 1.92 (d, $J = 12.5$ Hz, 2H), 2.10 (d, $J = 10.6$ Hz, 2H), 3.36 (d, $J = 2.7$ Hz, 1H), 3.48–3.57 (m, 10H), 4.27–4.29 (m, 2H), 4.42 (d, $J = 2.4$ Hz, 1H), 5.99 (d, $J = 2.0$ Hz, 2H), 6.16–6.17 (m, 1H), 6.61 (d, $J = 2.3$ Hz, 1H), 6.69 (d, $J = 2.0$ Hz, 1H), 6.86 (d, $J = 8.6$ Hz, 2H), 6.94 (d, $J = 9.0$ Hz, 2H); ^{13}C-NMR (100 MHz, CD_3OD) δ 26.0, 28.0, 48.3, 49.9, 51.2, 52.3, 57.1, 65.1, 67.0, 67.0, 100.7, 102.4, 107.3, 111.1, 115.7, 129.3, 136.4, 138.1, 140.1, 143.2, 157.3, 158.2, 159.9, 160.0, 160.9, 208.6; ESIMS *m/z*: 559.3 $(M+H)^+$; $C_{30}H_{41}NO_9$: HRMS calcd. 559.2776 $(M+H)^+$, found 559.2789.

5-Hydroxy-2-(4-hydroxyphenyl)-3-(4-(2-(piperidin-1-yl)ethoxy)phenyl)-2,3-dihydro-1H-inden-1-one (7a) Brown solid, yield 67%. mp: 234–235 °C; IR (film) 3321, 2932, 1745, 1633, 1521, 1499, 1451, 1354, 1320, 1212, 1147, 1110, 1027 cm^{-1}; ^{1}H-NMR (400 MHz, CD_3OD) δ 1.52–1.57 (m, 1H), 1.75–1.85 (m, 3H), 1.95 (d, $J = 14.8$ Hz, 2H), 3.02–3.08 (m, 2H), 3.54 (t, $J = 4.7$ Hz, 2H), 3.59 (s, 1H), 3.63 (d, $J = 4.4$ Hz, 2H), 4.32–4.35 (m, 2H), 4.39 (d, $J = 4.5$ Hz, 1H), 6.54 (d, $J = 1.1$ Hz, 1H), 6.71 (d, $J = 8.6$ Hz, 2H), 6.86 (d, $J = 8.6$ Hz, 2H), 6.90–6.92 (m, 1H), 6.96 (d, $J = 8.6$ Hz, 2H), 7.07 (d, $J = 8.6$ Hz, 2H), 7.67 (d, $J = 8.2$ Hz, 1H); ^{13}C-NMR (150 Hz, $CDCl_3$) δ 197.5, 161.5, 157.0, 141.3, 139.9, 137.9, 137.7, 136.9, 136.6, 129.3, 123.9, 123.5, 123.3, 122.5, 122.1, 121.0, 106.5, 95.8, 55.2, 54.9, 34.3, 20.8. HRMS calcd. 444.2169 $(M+H)^+$, found 444.2165.

3-(4-(2-(3,4-Dihydroisoquinolin-2(1H)-yl)ethoxy)phenyl)-5-hydroxy-2-(4-hydroxyphenyl)-2,3-dihydro-1H-inden-1-one (7b) Brown solid, yield 67%. mp: 215–216 °C; IR (film) 3356, 2937, 1806, 1623, 1511, 1476, 1344, 1320, 1276, 1201, 1157, 1133, 1021, 1026, 786, 577 cm^{-1}; ^{1}H-NMR (400 MHz, CD_3OD) δ 3.23 (m, 2H), 3.30 (m, 2H), 3.63 (d, $J = 5.2$ Hz, 1H), 3.74 (t, $J = 4.4$ Hz, 2H), 4.39 (d, $J = 4.8$ Hz, 1H), 4.44 (t, $J = 4.4$ Hz, 2H), 6.55 (s, 1H), 6.71(d, $J = 8.4$ Hz, 2H), 6.86 (d, $J = 8.4$ Hz, 2H), 6.91 (dd, $J = 8.4$ Hz, $J = 2$ Hz, 1H), 7.00 (d, $J = 8.4$ Hz, 2H), 7.20 (d, $J = 7.6$ Hz, 1H), 7.26–7.34 (m, 3H), 7.67 (d, $J = 8.4$ Hz, 1H); ^{13}C-NMR (100 MHz, CD_3OD) δ 26.0, 48.4, 49.6, 51.4, 54.7, 55.5, 55.6, 56.1, 63.0, 63.2, 65.7, 112.9, 116.1, 116.5, 118.0, 127.9, 128.3, 129.6, 129.9, 130.3, 130.9, 137.4, 157.7, 158.2, 161.6, 166.5, 206.5; HRMS calcd. 492.2169 $(M+H)^+$, found 492.2165.

5-Hydroxy-2-(4-hydroxyphenyl)-3-(4-(2-morpholinoethoxy)phenyl)-2,3-dihydro-1H-inden-1-one (7c) Brown solid, yield 45%. mp: 211–212 °C; IR (film) 3345, 2930, 1710, 1623, 1450, 1332, 1323, 1162, 1132, 1078, 1076, 690, 532 cm^{-1}; ^{1}H-NMR (400 MHz, CD_3OD) δ 2.02 (m, 2H), 2.15 (m, 2H), 3.19 (m, 2H), 3.61 (t, $J = 4.8$ Hz, 3H), 4.28 (t,

$J = 4.8$ Hz, 2H), 4.37 (d, $J = 4.8$ Hz, 1H), 6.52 (s, 1H), 6.69 (d, $J = 8.4$ Hz, 2H), 6.84 (d, $J = 8.4$ Hz, 2H), 6.89 (d, $J = 8.4$ Hz, 1H), 6.95 (d, $J = 8.4$ Hz, 2H), 7.05 (d, $J = 8.4$ Hz, 2H), 7.65 (d, $J = 8.4$ Hz, 1H); ^{13}C-NMR (100 MHz, CD_3OD) δ 21.9, 28.7, 46.6, 47.4, 53.2, 53.6, 53.7, 62.3, 63.7, 110.9, 114.1, 114.5, 116.0, 124.8, 127.0, 128.2, 128.5, 129.0, 135.3, 155.6, 156.3, 159.6, 164.4, 204.5; HRMS calcd. 446.1962 $(M+H)^+$, found 446.1965.

5-Hydroxy-2-(4-hydroxyphenyl)-3-(4-(2-(pyrrolidin-1-yl) ethoxy)phenyl)-2,3-dihydro-1H-inden-1-one (7d) Brown solid, yield 52%. mp: 214–215 °C; IR (film) 3347, 3001, 2946, 2852, 1711, 1627, 1490, 1411, 1352, 1320, 1210, 1142, 1078, 805, 773 cm^{-1}; ^{1}H-NMR (400 MHz, CD_3OD) δ 3.49 (m, 2H), 3.62 (m, 3H), 3.85–3.99 (m, 6H), 4.37 (m, 3H), 6.54 (s, 1H), 6.70 (d, $J = 8.4$ Hz, 2H), 6.85 (d, $J = 8.4$ Hz, 2H), 6.91 (d, $J = 8.4$ Hz, 1H), 6.96 (d, $J = 8.4$ Hz, 2H), 7.06 (d, $J = 8.4$ Hz, 2H), 7.67 (d, $J = 8.4$ Hz, 1H); ^{13}C-NMR (100 MHz, CD_3OD) δ 28.7, 47.9, 51.8, 53.6, 55.5, 60.9, 62.9, 63.7, 110.9, 114.1, 114.6, 116.0, 124.8, 127.0, 128.2, 128.5, 129.0, 135.3, 155.6, 156.1, 159.6, 164.5, 204.5; HRMS calcd. 430.2013 $(M+H)^+$, found 430.2010.

General procedure for the synthesis of 2-(3,5-dimethoxyphenyl)-4,6-dimethoxy-3-(4-(2-(aminoalkyl -1-yl) ethoxy)phenyl)-2,3-dihydro-1H-inden-1-ones (6a–b) and 5-methoxy-2-(4-methoxyphenyl)-3-(4-(2- (aminoalkyl-1-yl) ethoxy)-phenyl)-2,3-dihydro-1H-inden-1-ones (8a–d)

To an ice-cold solution of **18a–d** or **17a** or **17d** (1 mmol) in CH_2Cl_2 (20 mL), $BF_3{\cdot}OEt_2$ (0.2 mL) was dropwise added via syringe. After stirred at room temperature for 72–120 h under N_2 protection, the reaction was quenched with water (1–2 mL) and CH_2Cl_2 was evaporated. Then saturated sodium bicarbonate solution was added to the mixture. The resulting solution was extracted with ethyl acetate and organic phase was washed with brine and dried over Na_2SO_4. After evaporated the solvent, the residue was further purified by reversed phase silica gel column chromatography ($CH_3CN/H_2O/TFA = 1: 2: 0.1\%$) to give the desired product as yellowish or brown solid.

2-(3,5-Dimethoxyphenyl)-4,6-dimethoxy-3-(4-(2-(piperidin-1-yl)ethoxy)-phenyl)-2,3-dihydro-1H-inden-1-one (6a) Yellowish solid, yield 75%. mp: 212–213 °C; IR (film) 3369, 2919, 1724, 1621, 1493, 1352, 1311, 1202, 1130, 670, 498 cm^{-1}; ^{1}H-NMR (400 MHz, CD_3OD) δ 1.40–2.10 (m, 6H), 2.82–2.88 (m, 2H), 3.42 (s, 2H), 3.54 (s, 1H), 3.62 (s, 3H), 3.70 (s, 6H), 3.74 (s, 1H), 3.79 (s, 1H), 3.84 (s, 3H), 4.42 (s, 2H), 4.47 (d, $J = 1.9$ Hz, 1H), 6.19 (s, 2H), 6.33 (s, 1H), 6.66 (s, 1H), 6.75 (d, $J = 8.2$ Hz, 2H), 6.86 (s, 1H), 6.90 (d, $J = 8.6$ Hz, 2H); ^{13}C-NMR (150 Hz, $CDCl_3$) δ 196.4, 156.2, 152.3, 149.6, 140.8, 138.2, 137.9, 135.8, 129.2, 128.8, 128.5, 126.8, 123.2, 106.8, 103.4, 78.7, 55.7, 55.5, 40.6, 20.7, 20.3.HRMS calcd. 532.2694 $(M+H)^+$, found 532.2694.

2-(3,5-Dimethoxyphenyl)-4,6-dimethoxy-3-(4-(2-(4-methyl-piperidin-1-yl)-ethoxy)phenyl)-2,3-dihydro-1H-inden-1-one (6b) Brown solid, yield 62%. mp: 201–202 °C; IR (film) 3337, 3011, 2935, 1716, 1622, 1473, 1454, 1347, 1328, 1233, 1136, 1029, 730, 569 cm^{-1}; ^{1}H-NMR (400 MHz, CD_3OD) δ 1.25–1.42 (m, 8H), 2.13 (t, $J = 6$ Hz, 2H), 2.81 (t, $J = 6$ Hz, 2H), 3.01 (d, $J = 11.6$ Hz, 2H), 3.60 (d, $J = 2.8$ Hz, 1H), 3.65 (s, 3H), 3.73 (s, 6H), 3.87 (s, 3H), 4.09 (t, $J = 5.6$ Hz, 2H), 4.49 (d, $J = 2.8$ Hz, 1H), 6.22 (d, $J = 2.4$ Hz, 2H), 6.35 (t, $J = 2$ Hz, 1H), 6.68 (d, $J = 2$ Hz, 1H), 6.77 (d, $J = 8.8$ Hz, 2H), 6.88 (d, $J = 2$ Hz, 1H), 6.91 (d, $J = 8.8$ Hz, 2H); ^{13}C-NMR (100 MHz, $CDCl_3$) δ 14.0, 21.5, 22.6, 29.3, 29.6, 30.1, 31.8, 50.8, 54.1, 55.1, 55.2, 55.5, 55.7, 57.1, 65.1, 65.2, 76.7, 77.0, 77.3, 96.3, 98.8, 105.9, 106.5, 114.4, 127.9, 135.6, 138.3, 138.4, 141.4, 157.0, 157.6, 160.9, 161.8, 205.3; HRMS calcd. 546.2850 $(M+H)^+$, found 546.2854.

5-Methoxy-2-(4-methoxyphenyl)-3-(4-(2-(piperidin-1-yl) ethoxy)phenyl)-2,3-dihydro-1H-inden-1-one (8a) Yellowish solid, yield 82%. mp: 236–237 °C; IR (film) 3338, 3001, 1942, 1716, 1646, 1556, 1487, 1439, 1354, 1236, 1200, 1147, 1036, 1029, 850, 468 cm^{-1}; ^{1}H-NMR (400 MHz, CD_3OD) δ 1.37–1.77 (m, 6H), 2.96 (s, 2H), 3.42–3.61 (m, 5H), 3.74 (s, 3H), 3.77 (s, 3H), 4.27 (s, 2H), 4.34 (d, $J = 4.7$ Hz, 1H), 6.63–7.31 (m, 9H), 7.74–7.82 (m, 2H); ^{13}C-NMR (100 MHz, $CDCl_3$) δ 23.4, 25.0, 53.8, 54.3, 54.6, 55.1, 57.1, 63.7, 65.0, 108.9, 113.6, 114.3, 115.8, 125.1, 125.2, 128.3, 128.7, 128.9, 130.4, 134.1, 157.2, 158.0, 158.7, 165.2, 203.3; HRMS calcd. 472.2482 $(M+H)^+$, found 472.2487. We separated **8a** with HPLC and chiral column to give (2*S*,3*S*)-**8a** ($[\alpha]_D^{20} = +151.5$ ($c = 0.4$ in MeOH)) and (2*R*,3*R*)-**8a** ($[\alpha]_D^{20} = -151.5$ ($c = 0.4$ in MeOH).

5-Methoxy-2-(4-methoxyphenyl)-3-(4-(2-(4-methylpiperi-din-1-yl)ethoxy)-phenyl)-2,3-dihydro-1H-inden-1-one (8b) Yellowish solid, yield 82%. mp: 200–201 °C; IR (film) 3356, 2913, 1716, 1638, 1487, 1446, 1352, 1334, 1200, 1142, 1056, 1027, 668, 542 cm^{-1}; ^{1}H-NMR (400 MHz, CD_3OD) δ 0.94 (d, $J = 4.4$ Hz, 3H), 1.45 (s, 2/H), 1.67 (s, 2/H), 2.32 (t, $J = 10.8$ Hz, 2H), 2.97 (t, $J = 5.2$ Hz, 2H), 3.16 (d, $J = 10.8$ Hz, 2H), 3.67 (d, $J = 4.8$ Hz, 1H), 3.76 (s, 3H), 3.80 (s, 3H), 4.21 (t, $J = 5.2$ Hz, 2H), 4.37 (d, $J = 4.4$ Hz, 1H), 6.66 (s, 1H), 6.81–6.84 (m, 4H), 6.97–6.99 (m, 5H), 7.79 (d, $J = 8.8$ Hz, 1H); ^{13}C-NMR (100 MHz, $CDCl_3$) δ 20.4, 29.1, 53.8, 54.6, 55.1, 63.6, 64.3, 85.9, 108.8, 112.3, 113.7, 114.3, 115.3, 115.8, 125.1, 127.2, 128.5, 128.7,

130.3, 130.4, 131.5, 158.1, 158.5, 165.3, 203.0; HRMS calcd. 486.2639 $(M+H)^+$, found 486.2643.

3-(4-(2-(4-Cyclohexylpiperazin-1-yl)ethoxy)phenyl)-5-methoxy-2-(4-methoxyphenyl)-2,3-dihydro-1H-inden-1-one (8c) Yellowish solid, yield 82%. mp: 207–208 °C; IR (film) 3368, 2914, 1716, 1637, 1455, 1429, 1346, 1300, 1217, 1210, 1147, 1033, 754 cm^{-1}; ^{1}H-NMR (400 MHz, CD_3OD) δ 1.11–1.39 (m, 8H), 1.47 (d, $J = 10.4$ Hz, 2H), 1.69 (d, $J = 15.6$ Hz, 1H), 1.91 (d, $J = 12.0$ Hz, 2H), 2.25 (s, 2H), 2.90 (s, 2H), 3.08 (s, 4H), 3.60 (d, $J = 4.8$ Hz, 1H), 3.77 (s, 3H), 3.81 (s, 3H), 4.08 (s, 2H), 4.36 (d, $J = 4.8$ Hz, 1H), 6.66 (s, 1H), 6.81–6.84 (m, 4H), 6.98–7.03 (m, 5H), 7.79 (d, $J = 8.8$ Hz, 1H); ^{13}C-NMR (100 MHz, $CDCl_3$) δ 24.4, 26.1, 29.1, 47.6, 49.2, 52.8, 53.7, 54.7, 55.1, 55.7, 63.7, 65.1, 108.9, 113.7, 114.3, 115.7, 125.1, 128.4, 128.7, 128,9, 130.4, 158.1, 158.6, 165.2, 203.1; HRMS calcd. 555.3217 $(M+H)^+$, found 555.3220.

5-Methoxy-2-(4-methoxyphenyl)-3-(4-(2-morpholinoethoxy)phenyl)-2,3-dihydro-1H-inden-1-one (8d) Yellowish solid, yield 76%. mp: 217–218 °C; IR (film) 3357, 3003, 2937, 1715, 1622, 1583, 1479, 1446, 1335, 1227, 1216, 1178, 1146, 1008, 1026, 751, 512 cm^{-1}; ^{1}H-NMR (400 MHz, CD_3OD) δ 3.07 (s, 2H), 3.52 (s, 2H), 3.65 (d, $J = 4.8$ Hz, 1H), 3.70 (s, 2H), 3.77 (s, 3H), 3.81 (s, 3H), 3.98 (s, 4H), 4.36–4.38 (m, 3H), 6.65 (s, 1H), 6.79–6.84 (m, 4H), 6.91–7.01 (m, 5H), 7.79 (d, $J = 8.8$ Hz, 1H); ^{13}C-NMR (100 MHz, $CDCl_3$) δ 28.5, 52.0, 54.4, 55.2, 55.5, 62.4, 63.3, 70.4, 73.7, 81.7, 93.6, 100.5, 108.0, 112.3, 113.1, 113.6, 113.7, 131.4, 131.6, 132.0, 132.0, 187.6, 211.3; HRMS calcd. 474.2275 $(M+H)^+$, found 474.2278.

Cell culture

MCF-7 and MDA-MB-231 cell lines were obtained from Chinese Academy of Sciences. MCF-7 cell lines were cultured in RPMI1640 (HyClone Life technologies), supplemented with 10% (v/v) heat-inactivated fetal bovine serum (FBS) as well as 1% (v/v) penicillin and streptomycin (P/S). MDA-MB-231 cell lines were cultured in Dulbecco's modified Eagle's medium (DMEM) (HyClone Life technologies) cell culture medium supplemented with 10% FBS and 1% penicillin and streptomycin. All cell lines were maintained in a humidified atmosphere of 5% CO_2 at 37 °C.

Western blot analysis

The expression pattern of ER was confirmed by western blot analysis. MCF-7, MDA231 were purchased from American Type Culture Collection (ATCC) and cultured according to the supplier's recommendations, supplemented with 10% FBS and antibiotics. Cells were collected and washed twice with phosphate-buffered saline (PBS). After trypsin digestion, the centrifuged supernatant was discarded. Cell precipitations were lysed with 1 × LDS Sample buffer (Life Technologies, USA). For analysis, 20 μg of protein were resolved on 10% sodium dodecyl sulphate-polyacrylamide gel. After electrophoresis, the gel was transferred into "sandwich", and applied 180 mA for 120 min. After transfer membrane, polyvinylidene difluoride membrane was rinsed in TBST three times every 10 min. The membrane was placed in TBS/T blocking buffer containing 5% (w/v) skimmed milk powder and shaken for 1 h at room temperature. And the membrane was followed by overnight incubation with appropriate dilution of primary antibody: ERα (Cell Signaling Technology, USA), ERβ (Proteintech, USA) and β-actin (Bioworld Technology, USA). Protein bands were detected using Immobilon Western Chemiluminescent HRP Substrate (MILLIPORE, USA) and visualized using an image analyzer (BIO-RAD, USA).

Cell cytotoxicity assay

Cytotoxicity was measured using a MTT assay. MCF-7 and MDA-MB-231 cells were seeded into flat-bottomed 96-well microplates for 24 h and followed by the treatment of tamoxifen, raloxifene, isopaucifloral F and synthesized isopaucifloral F derivatives dissolved in dimethyl sulfoxide (DMSO) (100, 50, 25, 12.5, 6.25, 3.62, 1.81 μM as concentration gradient). After treatment, cell viability was assessed using the MTT method. The cytotoxicity assays were performed in triplicate.

Radiometric competitive receptor–ligand binding assay

The competitive binding assay method was performed as previously study described with slightly modification (Gim et al. 2014). The recombinant human ER (1.28 nM) was incubated with test compounds for 20 min at 4 °C in the presence of 5 nM of [2,4,6,7-^{3}H]-E2 (81.0 ci/mmol). Then 50% (v/v) hydroxyapatite PBS slurry (100 μL) was added to the reaction mixture. After sufficiently mixing, the mixture was kept for 15 min at 4 °C. Bound and free radioligand were separated by centrifugation at 12,000 × g for 2 min, and the radioactivity of the supernatant was determined using a liquid scintillation counter (LS-6500, Beckman counter, CA, USA). The amount of the receptor-bound [^{3}H]-E2 in the presence of the test compounds was presented relative to maximum receptor-bound ligand (2×10^{-8} M E2). The data are expressed as the ratio of the receptor-bound [^{3}H]-E2 in the presence of the compounds to the 0.1% DMSO used as a control.

Cell circle analysis

MCF-7 cells were plated in six-well plate and allowed to grow overnight. Then the cells were incubated with compound (2*R*, 3*R*)-**8a** at concentrations of 6, 12, and 18 μM for 48 h. Then untreated and treated cells were harvested, washed with PBS, fixed in ice-cold 70% ethanol, and stained with propidium iodide (Beyotime). Cell cycle analysis was performed by flow cytometry (FACScan, BD Biosciences, USA).

Evaluation of apoptosis with flow cytometry

MCF-7 cells were plated in six-well plate and allowed to grow overnight. The medium was then replaced and cells were treated with desired concentrations of lead compounds for 72 h. Cells treated with vehicle (0.001% DMSO in culture medium) were included as controls for all experiments. After 24 h of treatment, cells from supernatant and adherent monolayer cells were harvested by trypsinization and washed with PBS at 300 g. After that, the cells were stained with Annexin V-FITC and propidium iodide using the Annexin V-PI apoptosis detection kit (Beyotime). Flow cytometry was performed using a FACScan (Becton Dickinson) equipped with a single 488-nm argon laser. Annexin V-FITC was analyzed using excitation and emission settings of 488 and 535 nm (FL-1channel) whereas PI was recorded with 488 and 610 nm (FL-2 channel). Debris and clumps were gated out using forward and orthogonal light scatter.

Uterine wet weight assay and morphometric analysis

The protocol employed here was approved by the Local Ethics Committee for Animal Experiments at Fudan University. An OVX mice model was used. Thirty healthy female kunming mouse (Sippr/BK, Shanghai, China) weighing 30–40 g were housing in the specific pathogen free animal facilities under controlled conditions (temperature 21 ± 1 °C; relative humidity 50 ± 10%; 12:12 h light–dark cycle). After acclimatization to laboratory conditions for 10 days, the mouse were randomly assigned to five groups of six mouse: a sham-operated group (in which only a piece of fat around the ovary was ablated) and four groups of OVX mouse, including the placebo (OVX + NS), the positive control (OVX + tamoxifen, 0.1 mg/kg), low dosage group (OVX + (2*R*,3*R*)-**8a**, 0.1 mg/kg) and high dosage group (OVX + (2*R*,3*R*)-**8a**, 1 mg/kg). Oral administration of samples was performed once daily for 3 days. Animals were weighted and killed 24 h after the final treatment. The uterus was transected at the border of the cervix and stripped of extraneous connective tissue and fat. Whole-uterine weights were recorded (wet weight) and the uterine was placed in 10% neutral buffered formalin to fix for histological preparation. After fixed for over 48 h, paraffin embedding, 5 μm sectioning, mounting, and hematoxylin and eosin staining were completed by Shanghai Liqi Biological according to standard techniques. Morphometric analysis was performed using Scion Image analysis software (Scioncorp, Frederick, MD). Histological markers of uterotrophy, including LECH, luminal circumference and number of endometrial glands were quantified for each slide.

In vitro metabolic stability studies

Compound (2*R*,3*R*)-**8a** was incubated at a concentration of 20 μM with rat liver microsomes and NADPH (10 mM) at 37 °C for 60 min. The reaction was quenched by addition of four volume of acetonitrile at 0 and 60 min. After quenching by acetonitrile, samples were vortexed for 60 s and centrifuged at 12000 rpm for 5 min. The supernatant was injected into HPLC. Peak areas of test compounds at 0 and 60 min incubation were used to calculate the % remaining values with the formula: %Remaining = Peak $\text{Area}_{60\text{min}}$/Peak $\text{Area}_{0\text{min.}}$ $T_{1/2}$ and CL_{int} was calculated by the standard formula (Li et al. 2007).

$$T_{1/2} = \frac{Ln2}{k_e} = \frac{0.693}{k_e}$$

$$CL_{int} = \frac{0.693}{In\ vitro\ T_{1/2}} \cdot \frac{1}{\frac{mg}{mL} microsomal\ protein\ in\ reaction\ system}$$

Conclusions

In conclusion, we have designed and synthesized 16 isopaucifloral F (Jordan 2004) derivatives, and their potencies of breast cancer inhibition were evaluated. The ERα/β LBD-binding affinity of these compounds were also examined. Among them, (2*R*,3*R*)-**8a** demonstrated significant binding affinity and high ERα/β LBD selectivity. Through chiral resolution, it was found that (2*R*,3*R*)-**8a** displayed good antiproliferative propriety against human breast cancer cell lines MCF-7 (ERα+/β+) and MDA-MB-231 (ERα−/β+) than both positive controls tamoxifen and raloxifene. Besides, it also showed the trend to induce apoptosis in human breast cancer cell line MCF-7. Moreover, (2*R*,3*R*)-**8a** was demonstrated both significant binding affinity and good ERα/β LBD selectivity. Molecular docking analysis further confirmed specific interactions with ERβ-binding pocket. In addition, (2*R*,3*R*)-**8a** exhibited no uterine stimulation in the uterotrophic assay. As a result, (2*R*,3*R*)-**8a** could be a promising lead compound for future exploration of selective ERβ anti-breast cancer agents. Further evaluation of (2*R*,3*R*)-

8a in vivo anticancer experiments and development of its chiral synthetic method are ongoing in our laboratory.

Acknowledgements This work was supported by the National Natural Science Foundation of China (No: 81673297), Shanghai Municipal Committee of Science and Technology (No: 17JC1400200, 17431902500), and China Postdoctoral Science Foundation (BX20180065).

Funding The funders had no role in the design of the study; in the collection, analyses, or interpretation of data; in the writing of the manuscript, or in the decision to publish the results.

Author contributions Conceptualization and methodology, X.S., C.Z., and X.-X.L.; software, X.-X.L. and Y.T.; validation, X.-X.L.; formal analysis, X.-X.L.; investigation, X.-X.L.; resources, X.S.; data curation, X.-X.L.; writing—original draft preparation, X.-X.L.; writing—review and editing, X.S., J.-M.Y. and M.-L.T.; supervision, X.S.; project administration, X.-X.L.; funding acquisition, X.S.

Compliance with ethical standards

Conflict of interest The authors declare that they have no conflict of interest.

Publisher's note: Springer Nature remains neutral with regard to jurisdictional claims in published maps and institutional affiliations.

References

Bishayee A. (2009) Cancer prevention and treatment with resveratrol: from rodent studies to clinical trials. Cancer Prev Res (Phila). 2:409–418

Bray F, Ferlay J, Soerjomataram I, Siegel RL, Torre LA, Jemal A (2018) Global cancer statistics 2018: GLOBOCAN estimates of incidence and mortality worldwide for 36 cancers in 185 countries. CA Cancer J Clin. 68:394–424

Dotzlaq H (1997) Expression of estrogen receptor in human breast tumors. J Clin Endocrinol Metab. 82:2371–2374

Ellis AJ, Hendrick VM, Williams R, Komm BS (2015) Selective estrogen receptor modulators in clinical practice: a safety overview. Expert Opin Drug Saf. 14:921–934

Figueroa-Magalhães MC, Jelovac D, Connolly R, Wolff AC (2014) Treatment of HER2-positive breast cancer. Breast (Edinburgh, Scotland). 23:128–136

Fong CJ, Burgoon LD, Williams KJ, Forgacs AL, Zacharewski TR (2007) Comparative temporal and dose-dependent morphological and transcriptional uterine effects elicited by tamoxifen and ethynylestradiol in immature, ovariectomized mice. BMC Genomics. 8:151

Fox EM, Davis RJ, Shupnik MA (2008) ERbeta in breast cancer-onlooker, passive player, or active protector? Steroids. 73:1039–1051

Gim HJ, Li H, Jung SR, Park YJ, Ryu JH, Chung KH, Jeon R (2014) Design and synthesis of azaisoflavone analogs as phytoestrogen mimetics. Eur J Med Chem. 85:107–118

Grese TA, Sluka JP, Bryant HU, Cullinan GJ, Glasebrook AL, Jones CD, Matsumoto K, Palkowitz AD, Sato M, Termine JD, Winter MA, Yang NN, Dodge JA. 1997 Molecular determinants of tissue selectivity in estrogen receptor modulators. Proc Natl Acad Sci USA. 94:14105–14110

Hao XD, Chang J, Qin BY, Zhong C, Chu ZB, Huang J, Zhou WJ, Sun X (2015) Synthesis, estrogenic activity, and anti-osteoporosis effects in ovariectomized rats of resveratrol oligomer derivatives. Eur J Med Chem. 102:26–38

Hartman J, Strom A, Gustafsson JA (2009) Estrogen receptor beta in breast cancer-diagnostic and therapeutic implications. Steroids. 74:635–641

Howell A, Evans DG (2013) Breast cancer prevention: SERMs come of age. Lancet. 381:1795–1797

Jordan VC (2004) Selective estrogen receptor modulation: concept and consequences in cancer. Cancer Cell. 5:207–213

Khamis AAA, Ali EMM, El-Moneim MAA, Abd-Alhaseeb MM, El-Magd MA, Salim EI (2018) Hesperidin, piperine and bee venom synergistically potentiate the anticancer effect of tamoxifen against breast cancer cells. Biomed Pharmacother. 105:1335–1343

Li HY, Sun J, He ZG (2007) In vitro prediction of in vivo hepatic metabolic clearance of drugs in human. Chin J New Drugs and Clin Remedies. 26:702–707

Lipinski CA, Lombardo F, Dominy BW, Feeney PJ (2001) Experimental and computational approaches to estimate solubility and permeability in drug discovery and development settings. Adv Drug Deliv Rev. 46:3–26

Luo HF, Zhang LP, Hu CQ (2001) Five novel oligostilbenes from the roots of Caragana sinica. Tetrahedron. 57:4849–4854

Ma DY, Luo HF, Hu CQ (2010) Three stilbene tetramers from the roots of Caragana sinica. Chin J Chem. 22:207–211

Mak P, Leung YK, Tang WY, Harwood C, Ho SM (2006) Apigenin suppresses cancer cell growth through ERbeta. Neoplasia. 8:896–904

Meri De Angelis FS, Kathryn AC, Benita S, Katzenellenbogen BS, Katzenellenbogen JA(2005) Indazole estrogens: highly selective ligands for the estrogen receptor beta J Med Chem. 48:1132–1144

Mosselman S, Polman J, Dijkema R (1996) ERβ: Identification and characterization of a novel human estrogen receptor. FEBS Lett 392:49–53

Paterni I, Granchi C, Katzenellenbogen JA, Minutolo F (2014) Estrogen receptors alpha (ERalpha) and beta (ERbeta): subtype-selective ligands and clinical potential. Steroids. 90:13–29

Skliris GP, Leygue E, Watson PH, Murphy LC (2008) Estrogen receptor alpha negative breast cancer patients: estrogen receptor beta as a therapeutic target. J Steroid Biochem Mol Biol. 109:1–10

Ström A, Hartman J, Foster JS, Kietz S, Wimalasena J, Gustafsson JÅ (2004) Estrogen receptor β inhibits 17β-estradiol-stimulated proliferation of the breast cancer cell line T47D. Proc Natl Acad Sci USA 101:1566–1571

Sun X, Izumi KJ, Hu CQ, Lin GQ (2006) Convenient synthesis of indene derivatives via intramolecular friedel—crafts cyclization of tetraaryl substituted 1,3-butadienes. Cheminform. 37:430–434

Sun X, Zhu J, Zhong C et al. (2007) A concise and convenient synthesis of stilbenes via benzils and arylmethyldiphenylphosphine oxides. Chin J Chem 25:1866–1870

Tang ML, Peng P, Liu ZY, Zhang J, Yu JM, Sun X (2016) Sulfoxide-based enantioselective nazarov cyclization: divergent syntheses of (+)-Isopaucifloral F, (+)-Quadrangularin A, and (+)-Pallidol. Chemistry. 22:14535–14539

Tang ML, Zhong C, Liu ZY, Peng P, Liu XH, Sun X (2016) Discovery of novel sesquistilbene indanone analogues as potent anti-inflammatory agents. Eur J Med Chem 113:63–74

Wang M, Liu X, Zhou L, Zhu J, Sun X (2015) Fluorination of 2-substituted benzo[b]furans with Selectfluor™. Org Biomol Chem. 13:3190–3193

Zhong C, Liu XH, Hao XD, Chang J, Sun X (2013) Synthesis and biological evaluation of novel neuroprotective agents for paraquat-induced apoptosis in human neuronal SH-SY5Y cells. Eur J Med Chem. 62:187–198

Zhong C, Zhu J, Chang J, Sun X (2011) Concise total syntheses of (±) isopaucifloral F, (±)quadrangularin A, and (±)pallidol. Tetrahedron Lett 52:2815–2817

Zhu J, Zhong C, Lu HF, Li GY, Sun X (2008) Toward the synthesis of caraphenol C: substituent effect on the nazarov cyclization of 2-arylchalcones. Synlett 2008:458–462